

This is the author-created version of the following work:

**Wasson, Robert, Archarjee, Shukla, and Rakshit, Raghupratim (2022) *Towards identification of sediment sources, and processes of sediment production, in the Yarlung-Tsangpo Brahmaputra River catchment for reduction of fluvial sediment loads. Earth-Science Reviews, 226 .***

Access to this file is available from:

<https://researchonline.jcu.edu.au/72449/>

© 2022 Elsevier B.V. All rights reserved. Accepted author manuscript version is made available under the CC-BY-NC-ND 4.0 license  
<https://creativecommons.org/licenses/by-nc-nd/4.0/>

Please refer to the original source for the final version of this work:

<https://doi.org/10.1016/j.earscirev.2022.103932>

**Towards identification of sediment sources, and processes of sediment production, in the Yarlung-Tsangpo-Brahmaputra River catchment for reduction of fluvial sediment loads**

Robert Wasson a, e, \*, Shukla Acharjee b, Raghupratim Rakshit c, d

a College of Science and Engineering, James Cook University, 1/14-88 McGregor Rd., Smithfield, Queensland 4878, Australia

b Centre for Studies in Geography, Dibrugarh University, Dibrugarh 786004, Assam, India

c Department of Applied Geology, Dibrugarh University, Dibrugarh 786004, Assam, India

d Department of Geophysics, Pachhunga University College, Aizawl, Mizoram 796001, India

e Fenner School of Environment and Society, Australian National University, ACT 2601, Australia

Keywords: Brahmaputra River, Floods, Sediment sources, Soil conservation

## ABSTRACT

Sedimentation in the Brahmaputra River has led to the widening and shallowing of its channel, resulting in land loss and deposition on agricultural land, exacerbating floods, threatening the viability of flood mitigation embankments, and could even lead to the riverbed becoming higher than the floodplain over much of its length with potentially disastrous consequences when embankments breach. To reduce channel sedimentation, by soil conservation it is first necessary to identify sediment sources. The aim of this paper is to review current knowledge of sources and the processes of sediment production, with a subsidiary benefit of providing a summary of the major geomorphic processes at work in the catchment. From the existing literature and a small amount of new analysis, the quantity of sediment being delivered to the River from major source regions has been identified showing that about 45% comes from the Yarlung-Tsangpo Gorge (in the northeast syntaxis), 40% from the Himalaya and the rest from the Mishmi hills, Indo-Burman Ranges and the Shillong Plateau. While the major sediment producing processes have been identified, insufficient information exists to quantify their relative importance. Similarly, sufficient information from regions within catchments does not exist to design a targeted soil conservation program. If further progress is to be made in identification of sediment sources, a spatially comprehensive strategy is needed. Such a strategy is described which would rely upon geochemical tracers rather than measurement of sediment fluxes. This approach has the advantage of gaining results relatively quickly and can be applied to the entire catchment once a pilot study has been completed and sufficient resources made available. If about half of the current rate of sedimentation in the river could be reduced, given that the sediment coming from the Gorge probably cannot be managed, this could help alleviate part of the land loss and flood problem suffered by the people of the lower catchment.

### 1. Introduction

Sedimentation in river channels can, inter alia, increase flood hazard by reducing the conveyance capacity for floodwaters, and therefore exacerbate overbank flows, and erode flood mitigation embankments along river margins by raising the level of flood flows. Also, if the rate of sedimentation on adjacent floodplains is lower than in channels, eventually the channel will become higher than its floodplain (a concern raised by Kingdon-Ward, 1955, for the Brahmaputra) under which circumstances flood mitigation embankments

will need to be raised (or abandoned) at considerable cost, or if embankments are retained any breach will produce very damaging floods. There are some examples of this phenomenon in Assam but the Yellow River (Huang He) in China is the iconic example where the present-day channel belt is up to 10 m above the floodplain and, despite super-human construction of embankments, the risk of an embankment breach remains, with potentially devastating consequences (Chen et al., 2012; Chen et al., 2018). To this should be added the prospect of increased sediment loads in the Brahmaputra as a consequence of climate change, by about 40% at Bahadurabad by 2075–2100 (Fischer et al., 2017) and by the 2090s by 52–60% (Darby et al., 2015). And floods may worsen; Ghosh and Dutta (2011) suggest that by the 2070s peak river flow will increase by about 28% because of climate change and by about 9% from plausible assumptions about land use change. Alam et al. (2021) suggest that annual maximum streamflow at Bahadurabad will increase by 22% by the end of the 21st Century. Increased peak flows will exacerbate flooding that may be increased by sedimentation. Glacial Lake Outburst Floods (GLOFs) and their transport of large amounts of sediment are also likely to become more frequent as the atmosphere warms (Gurung et al., 2017).

The Brahmaputra is one of many volatile flood-prone rivers overloaded with sediment that rises partially in the Himalaya, the other notable examples being the Kosi and the Bagmati rivers. But the present authors have experience of the Brahmaputra and have been exposed to the views of flood managers in the Assam Water Resources Department who have posited that channel sedimentation may be a serious problem because it exacerbates floods. The officers of this Department therefore are keen to learn about how to reduce channel sedimentation as part of their arsenal of methods for reducing flood impacts. Furthermore, the approach of this paper could be applied to other rivers in the region. Sediment sources need to be identified, particularly those that can be managed to reduce sediment fluxes, and a plan devised to build on what is already known. Once sediment sources have been identified a soil conservation and sediment transport reduction plan should be constructed, implemented, and monitored for effectiveness.

Only current knowledge of sediment sources and a plan to improve that knowledge is dealt with here because current knowledge of sources is insufficient. Information about sedimentation rates in the channel-floodplain system, and the extent to which embankments are starving floodplains of sediment, would also be useful for assessment of the potential for the channel bed to rise above the floodplain, but will not be considered here. It is of paramount importance that management plans for any or all these problems are based upon evidence because there has been a tendency in India and in many other countries to 'identify' sediment sources without evidence.

## 2. Materials and methods

The approach adopted here is to review and find links between existing published knowledge (most of which was not produced for this purpose) and observations and limited analyses by the authors, from a wide range of disciplines, including geology, geochemistry, seismology, geomorphology, hydrology, soil science, and remote sensing to provide as

complete a picture as possible of the current understanding of this extremely complex and dynamic region. The published material comes from the knowledge of the authors, information provided by others who have worked in the catchment, and from online search engines. It is recognized that there are differences in the resolution of the different data sources, but no attempt has been made to standardize results as this would require access to original data, much of which is not available. Therefore, reliance is placed upon the uncertainties provided in the original papers and comparison of different results from different methods.

The review and identification of connections and synergies between different bodies of knowledge is an important approach to the solution of any multifaceted problem. This paper focuses on the full range of sediment sources in the Brahmaputra River and its tributaries, along with processes and rates of sediment generation, opportunities for reduction of erosion and sediment delivery to rivers, future information needs, and a strategy for obtaining this information.

### 3. Climatic and tectono-geomorphic setting

The rainfall (a large part of the total precipitation) that drives river flow and much of the erosion in the Basin is dominated by the Southwest Monsoon, (Fig. 1) with a subordinate effect from the Northeast Monsoon (Fig. 2) and the Westerlies. Fig. 1 shows that the highest average totals from the Southwest Monsoon are along the Himalayan front between the Main Boundary Thrust and Main Central Thrust (Fig. 3) because of orographic processes, decreasing to the northeast into the Mishmi Hills and onto the eastern margin of the Tibetan Plateau (TP) where there is some influence from the East Asian Monsoon. Over most of the TP the precipitation is very low.

The collision of the Indian tectonic plate with the almost stationary Eurasian plate (including the Burma micro-plate) about 50 million years ago created the Himalayan mountain range which, at its eastern end, has an arcuate form (known as a syntaxis) with the boundary (or suture) between the two plates trending E-W in southeast Tibet, then bending by about 180° through the Namche Barwa-Gyala Peri Massif (NB-GP) before turning to the southeast and then to the south in western Myanmar. The syntaxis corresponds to the north-eastern indenter corner of the Indian plate, producing widespread deformation of rocks, by buckling of the crust, and seismicity (Bracciali et al., 2016). Tectonically active zones effectively surround the Brahmaputra valley, with the Himalaya on the northern side, the Mishmi Hills on the northeast, the Indo-Burman ranges to the east and southeast, and the Shillong Plateau and Mikir Hills to the southeast, all of which are seismic source zones (Bahuguna and Sil, 2018) (Fig. 3).

The Brahmaputra River rises on the Tibetan Plateau as the Yarlung- Tsangpo River that flows to the east along the suture between the Indian and Eurasian plates before turning through the syntaxis and falling to the Assam plain (Fig. 4) through a gorge with relief of about 5 km.

Modern erosion rates as high as 10 mm yr<sup>-1</sup> in the syntaxis are among the highest in the world, and rates of rock exhumation (unroofing of rock by tectonic and/or surficial processes; Ring et al., 1999), also up to 10 mm yr<sup>-1</sup>, are also among the highest globally with different rates depending on method, sample location, and the time period over which they are estimated (e.g., Bracciali et al., 2016).

The Brahmaputra River flows through the Assam valley that is about 100-110 km wide and bounded by tectonically mobile mountain belts. In the Himalayan thrust belt the Main Frontal Thrust (MFT; Burgess et al., 2012) and the Main Central Thrust (MCT) are the major faults, in the Mishmi Hills there are the Lohit and Mishmi Thrusts, and in the Indo-Burman Ranges are the Naga and Disang Thrusts (Angelier and Baruah, 2009). The Brahmaputra Riverbed falls from the edge of the TP about 2500 m over about 200 km through the Yarlung-Tsangpo Gorge. Locations along the long profile of this river are shown in Fig. 5. Many of the rivers rising in the Himalayan part of the catchment have very steep upper reaches, such as the Teesta (Fig. 6), a major tributary of the Brahmaputra. But none have the spectacular incised form of the Gorge.

#### 4. Channel sedimentation and dynamics

Data for this topic come from different parts of the river system over different time periods, thereby limiting firm conclusions. At Dibrugarh (Fig. 4) the Brahmaputra has widened since 1950 CE, but since about 1995 has not done so (Fig. 7 A 1). In Bangladesh, on the Jamuna River channel, width has consistently increased from 1973 to 2010 (Fig. 7 E 2). The Brahmaputra River is also aggrading, as inferred from High Flood Levels (HFL) at several gauging stations (Goswami, 1985) (Fig. 7 A 2). Trends in HFL values are consistent with specific gauge analysis (where flood stage for a specific discharge is analysed through time) for this river (Sarkar and Thorne, 2006). Therefore, HFL is used because for some stations it is the only available metric. The HFL record for the Teesta River (Fig. 7 B) is too short to detect a long-term trend, although it appears to have increased. Based on the analysis by Goswami, and more recent data from the Assam Water Resources Department (WRD) and earlier data from the then Public Works Department, the HFLs increased from 1913 (the earliest available record) until the mid 1980s during which time there has been no trend in peak discharges measured by the Central Water Commission at Dibrugarh (not shown, but see Wasson et al., 2020). At Pandu (Figs. 4 and 7D) the record is too short to detect a trend. In the mid 1980s peak discharges at Dibrugarh suddenly increased (not shown, but see Wasson et al., 2020), but the rate of increase of HFLs began to decline.

These out-of-phase relationships between HFL and peak discharges show that HFL reflects channel bed aggradation, typical of the behaviour of sediment waves (transient sediment fluxes) in contrast with channel bed waves (the rise and fall of a channel bed because of sedimentation) (James, 2010). In more detail, aggradation at Dibrugarh had an upward trend from 1913 to 1953 ( $p < 0.01$  using the non-parametric Kendall Tau (b) test, given that the Jarque-Bera Skewness-Kurtosis normality test shows that the data are non-normally distributed), at an average rate of 2.5 cm yr<sup>-1</sup> with a total bed level change of 1.3 m. The rate increased in 1954, and to 2015 the average rate was 3.3 cm yr<sup>-1</sup> with a total bed level change of 2.1 m. The rate of increase has declined since the early 1990s. WRD HFL data at Dholla (Fig. 2) on the Lohit River show a declining trend ( $p < 0.1$ ) to 2017 from the

earliest available data in 2006 (Fig. 7 A3). At Pandu, a little downstream of Guwahati, aggradation occurred from 1953 to 1963 during a period of high sediment transport, with a peak between about 1968 and 1970, and then fell to 1976 (not shown), a trend that Goswami (1985) interpreted to be a result of site-specific factors, although it could be a result of a damped oscillation; i.e., an oscillation that fades away over time. The braid index (a measure of channel multiplicity) at Pandu (Fig. 7C) has slightly increased along with width and aggradation at Dibrugarh. Between 1972 and 2002 the braid index in the Jamuna in Bangladesh increased (Fig. 7E) and has fallen since about 1996.

All scientific analyses of these trends in HFL, channel aggradation, and channel width and braid index increase have implicated the massive input to the river of landslide debris triggered by the 8.6 magnitude earthquake in 1950 in Upper Assam (Priyanka et al., 2017), a phenomenon personally observed by Kingdon-Ward (1955). Mathur (1953) reported an estimate for the amount of landslide sediment produced by the earthquake, from which it is estimated that about  $7.5 \times 10^{10}$  t was moved if it is assumed that only soil was entrained, although this is uncertain as a constant landslide depth was assumed and only a few calibration measurements were made (see Marc et al., 2016). The most severely affected area was in the upper Lohit, Siang and Dibang river catchments. Much of this sediment reached these rivers and the Brahmaputra and apparently caused the aggradation at Dibrugarh and Pandu. In the Jamuna River in Bangladesh around Bahadurabad (Fig. 4), Sarkar and Thorne (2006) show that a pulse of bedload arrived about eight years after the earthquake and the channel bed began to rise about two years later. The channel bed level reached a maximum about 16 years later and then began to decline according to their conceptual model. The decreasing rate of increase of the channel bed elevation at Dibrugarh and the declining level at Dholla suggest depletion of the landslide sediment, either by exhaustion of the sediment delivered to streams or revegetation of the landslide scars, while the decrease at Bahadurabad, and probably at Pandu, combined with the earlier rise and apparent stabilization at Dibrugarh and the fall of bed elevation at Dholla, suggests a damped oscillation as the sediment from the earthquake-induced landslides moved downriver (Fig. 7). The slowly increasing aggradation prior to the 1950 earthquake shows that the channel received more sediment than it can transport, and after 1950 this was even more the case, in a subsiding foreland basin that is rapidly filling with sediment (Borgohain et al., 2017).

Lupker et al. (2017) used the cosmogenic radionuclide  $^{10}\text{Be}$  in river sands to estimate the rate of total sediment (bedload and suspended load) transport in the Brahmaputra and tributaries, a technique that provides estimates averaged over centuries to millennia, the averaging time being in inverse proportion to the catchment denudation rate. At Dibrugarh the best estimate of the transport rate is provided by the mid-point of the band of estimates in Fig. 10 of Lupker et al. (2017) that is calculated by adding tributary inputs to the flux at the mountain front and which treats the outlier at Dibrugarh as an anomaly that could be a result of sediment waves from short-term pulses of erosion generated for example by large landslides east of Pasighat (M. Lupker, pers. comm., 2018), by the flood of 2000 (Shang et al., 2003), and/or by landslides along roads (Luirei and Bhakuni, 2008). Averaged over about 300 years the best estimate of total load at Dibrugarh is  $800 \pm 350 \times 10^6$  t yr<sup>-1</sup> as explained above. Assuming that the pre-1953 bed elevation increase at Dibrugarh of

2.5 cm yr<sup>-1</sup> (the background rate) continued at the same rate to 2015, then the change between 1953 and 2015 at an average of 3.3 cm yr<sup>-1</sup> consisted of 0.8 cm yr<sup>-1</sup> as a result of the 1950 earthquake. Using the results of Sarma and Acharjee (2018) and Lahiri and Sinha (2012), the annual deposition rate in Unit 1 of the latter authors (from the Lohit-Brahmaputra junction for a distance of 51 km downstream) before the earthquake was  $7.13 \times 10^6$  t yr<sup>-1</sup> and after the earthquake was  $23.78 \times 10^6$  t yr<sup>-1</sup>, meaning that  $16.66 \times 10^6$  t yr<sup>-1</sup> was a result of the earthquake. While the bed level rose by a factor of 1.3 above the background rate after the earthquake, the total deposition rate increased by a factor of 3.3 at Dibrugarh.

The same sets of processes are likely to have occurred following all great earthquakes in the catchment and because of intense and prolonged rainfall. In the Darjeeling Himalaya, part of the Teesta River catchment (part of the Brahmaputra catchment), large amounts of rain fell in 1899, 1950 and 1968. In 1968 large numbers of landslides led to the aggradation of the Teesta River from Teesta Bazar (Fig. 6) downstream (Starkel and Basu, 2000). The bed of the river rose by 5-6 m and since 1974 began to fall. From the earliest record in 1941 to 1953 the bed of the Teesta rose at a near-constant rate then suddenly rose as much as during the previous 13 years (Ray, 1956). The sudden rise was 3 years after the 1950 rainfall event superimposed on the steady rise which, analogous to the Brahmaputra prior to 1950, is likely to have been a response to high background catchment erosion rates in a subsiding foreland basin. If this is the case the time for relaxation to the background state, between 1899 and 1950, was less than 51 years, the time between these two events.

## 5. Riverine sediment fluxes

Goswami (1985) was the first to quantify the suspended load in the main river and its major tributaries. Between 1971 and 1977 the total specific suspended load at Tsela D'Zong on the Tibetan Plateau in the Yarlung-Tsangpo River was about  $13 \times 10^6$  t yr<sup>-1</sup> and increased at Ranaghat (2-3 km from Pasighat) to about  $210 \times 10^6$  t yr<sup>-1</sup> at the outlet of the Gorge, then further at Bessamara to about  $734 \times 10^6$  t yr<sup>-1</sup> with tributary inputs below Ranaghat (from the Dibang, Lohit, Burisuti, Burhi Dihing, Desang, Dikhow, and Jhanji and a few other rivers; Fig. 4) of about  $416 \times 10^6$  t yr<sup>-1</sup> or 57% of the total at Bessamara. About 43% of the total at Bessamara as measured at Ranaghat came from the syntaxis including the Gorge. Further downstream the annual suspended sediment yield fell to about  $160 \times 10^6$  t yr<sup>-1</sup> at Pandu and  $102 \times 10^6$  t yr<sup>-1</sup> at Jogighopa, results not found in other studies.

Goswami (1985) estimated the uncertainties in these numbers at <50%, although some were much lower than 50%. But the largest source of uncertainty is in the proportion of the total load that is bedload, a value that could not be calculated from the data available to Goswami, but it may be about the same as the suspended load (Stewart et al., 2008). Shi et al. (2017) have reported data from the Yarlung-Tsangpo River in Tibet, where a little upstream of the Gorge the mean annual suspended load was  $10.43 \times 10^6$  t yr<sup>-1</sup>, between 2007 and 2009, close to the estimate by Goswami (1985).



Partly because of the difficulty of measuring sediment fluxes, and bedload in particular, other investigations of sediment fluxes and sources have relied upon geochemical methods blended where necessary and possible with gauge-based estimates of sediment flux. Using a chemical mass balance approach Galy and France-Lanord (2001) and Singh (2006) estimated that the total sediment load is about twice the suspended load, meaning that bedload is about 50% of the total where the river enters Bangladesh. Garzanti et al. (2004) used petrographic data from deposited sand to show that  $42 \pm 12\%$  of the total sand load upstream of the Brahmaputra-Teesta junction comes from the Siang River and probably mainly from the NP-GP including the Gorge, given that the flux in the Yarlung-Tsangpo is small because of the Plateau's low relief, dry climate and sediment storage (Liang et al., 2021). An additional 25% comes from the Himalaya (some from that part crossed by the Siang River) and 20% from the Mishmi Hills (mainly from the Lohit River). Moreover, ~25% of the total sediment reaching the Bay of Bengal comes from the syntaxis, a remarkable contribution from an area of only a few percent of the total catchment area upstream of the Bay. A spatially more limited study by Stewart et al. (2008) used the U-Pb ages of detrital zircon grains in samples of deposited sand upstream of the syntaxis and at Pasighat downstream of the syntaxis to estimate that ~50% of the sediment deposited at Pasighat comes from the syntaxis. Cina et al. (2009), Zhang et al. (2012), and Lang et al. (2013) have also demonstrated significant dilution of the Tibetan Plateau zircons by sediment from the syntaxis. Enkelmann et al. (2011) combined the young zircon fission track cooling ages in the sands at Pasighat with Goswami's estimate of suspended load at the same site with a new and larger estimate of the area of high exhumation rates to calculate that 60–70% of the sediment load at Pasighat comes from the syntaxis of which 30–40% comes from the area downstream of the Gorge (Enkelmann pers. com., 2021). Singh and France-Lanord (2002) estimated the total sediment load from chemical and isotopic tracers (most usefully Sr isotopes and  $\epsilon\text{Nd}$ ) and a mixing equation that uses end member compositions of the major source terrains. Sampling of deposited sediment in the Brahmaputra from Pasighat to Chilmari and the major tributaries enabled calculation of inputs to the main river. The Siang River in the Gorge contributes  $81 \pm 25\%$  of the sediment flux at Dibrugarh,  $58 \pm 23\%$  at Guwahati and  $49 \pm 27\%$  at the furthest downstream sampling point. As already noted, Lupker et al. (2017) used  $^{10}\text{Be}$  to calculate denudation rates and from them total sediment fluxes from the mid-Yarlung-Tsangpo to close to the Bangladesh border. Samples from the Tibetan Plateau show that the sediment flux into the Gorge is about  $140 \times 10^6 \text{ t yr}^{-1}$  (from the Yarlung-Tsangpo, Yigong and Parlung rivers), averaged over millenia, about ten times the suspended load estimated by Shi et al. (2017) who used short gauged records and did not estimate the bedload fraction. From Lupker et al. (2017) at Pasighat the flux averages  $405 \pm 110 \times 10^6 \text{ t yr}^{-1}$ , although upstream at Pangin the flux is  $880 \pm 240 \times 10^6 \text{ t yr}^{-1}$ , between which sites there is little opportunity for deposition, suggesting that the system is not in steady state and the calculations in the syntaxis may not be reliable. This possibility is given more weight by results from Zhang et al. (2021) using both  $^{10}\text{Be}$  and  $^{26}\text{Al}$  suggesting a much lower denudation rate in the upper Gorge which they explain by exhumation of deeply buried sediment. This idea needs further examination. Gerignani et al. (2018) used petrographic data to show that sediment production in the syntaxis increases the contribution from the Yarlung-Tsangpo River by between 5 and 100 times, the erosion rate in the Siang River is higher than those in the Himalaya by 2–10 times, anomalously the Mishmi Hills

have low erosion rates, given their high relief and seismicity, and the signal from the syntaxis is diluted by inputs from the Himalayan rivers. Overall, their results agree with those of Lupker et al. (2017) but there are no results from the Indo-Burman Ranges for comparison. Gerignani et al. (2018) also calculated the sediment flux at Pasighat as  $397\text{--}583 \times 10^6 \text{ t yr}^{-1}$ , by combining results from Lupker et al. (2017) with their petrographic data. This range includes the estimates from Lupker et al. (2017) and Stewart et al. (2008), and the recalculated estimate of Goswami's (1985) results and represents 35–51% of the sediment flux near the junction with the Ganga (Table 1). The large degree of agreement between the  $^{10}\text{Be}$  and petrographic data suggests that the results are not dependent upon the different sediment size fractions used in the two studies.

As already noted, the recalculated modern sediment flux at Pasighat, based on Goswami (1985) and the addition of 50% bedload is about  $420 \times 10^6 \text{ t yr}^{-1}$ , an estimate that is indistinguishable from that based on  $^{10}\text{Be}$  when the uncertainties are considered. Lupker et al. (2017) argue however that theirs is an underestimate for reasons that they analyse in detail. At the most downstream sampling site (Tezpur and Yamuna bg.), just below the Teesta-Brahmaputra junction, the flux averaged over 300 to 600 years is  $1140 \pm 240 \times 10^6 \text{ t yr}^{-1}$ , an increase from Pasighat by a factor of about 2.7. The increased flux downstream of the mountain front at Pasighat is consistent with the input of sediment from the tributaries, the fluxes in which have been corrected by removing from the calculations the areas of catchments below 300 m ASL because, it is argued, there is no significant denudation in the lowland areas and reworking of sediment by laterally migrating channels has a very small effect on  $^{10}\text{Be}$  concentrations. Of the  $\sim 658 \times 10^6 \text{ t yr}^{-1}$  (about 58%) added to the Brahmaputra by the major tributaries some 22% comes from tributaries in the Mishmi Hills (Dibang, Lohit) and 36% from the northern bank (Subansiri, Kameng, Manas, Tsang Chhu, Teesta, all rising in the Himalaya). These results suggest that the amount of sediment produced in the syntaxis is likely to be about 30% if the input to the Gorge is accepted to be 12% (the sum of inputs from the Yigong, U Rong Chu and the Yarlung-Tsangpo), averaged over centuries to millennia. There is no account in these estimates for a contribution from the Indo-Burman Ranges. The Noa Dhing, Buri-Dihing and Desang rivers drain erodible Tertiary rocks in the Indo-Burman Ranges and may therefore carry high sediment loads. But the bulk sand petrography (Garzanti et al., 2004) shows that they contribute little sediment to the Brahmaputra suggesting that much of their sediment is deposited before reaching the main river. The same appears to be the case for the rivers draining the Shillong Plateau for which there are no measured or estimated loads, but which have no noticeable impact on the estimated loads in the Brahmaputra according to the results of Lupker et al. (2017).

## 6. Sediment sources, processes and rates of sediment generation

Depending upon the method (see Table 1), the syntaxis produces between 30 and 51% of the sediment in the river near where it enters Bangladesh, the most likely estimate being 45% from the results of Singh and France-Lanord (2002) for modern sediment, which overwhelms that from the Yarlung-Tsangpo on the TP. The remainder comes from the tributary streams downstream of the Gorge and the banks of the Brahmaputra. Therefore,

it is necessary to identify sediment sources and generating processes in the tributary catchments.

### 6.1. The Yarlung-Tsangpo catchment

Liang et al. (2021) used petrographic data, heavy minerals and geochemistry of modern sand bar samples from the middle to lower reaches of the Yarlung-Tsangpo River to show that  $77 \pm 9\%$  of the sand comes from the Lhasa Block (through the northern tributaries) and  $15 \pm 7\%$  comes from the Himalaya (through the southern tributaries). They also showed that  $13 \times 10^6$  t/year is deposited in the lower reaches which is more than the quantity delivered to the Gorge. This is consistent with the  $>500$  m of sediment deposited in this area over the past 2.5 to 2.0 Ma which is presently being incised near the confluence of the Yarlung-Tsangpo and Nyang River.

### 6.2. The Gorge

The syntaxis, including the Gorge, produces about 45% of the total modern flux in the Brahmaputra. The Gorge began to steepen after 1.5 million years ago (Salvi et al., 2017) as a consequence of rapid rock uplift during the convergence of the Indian and Eurasian tectonic plates, producing steep river gradients and adjoining hillslopes, stream power (the rate of energy dissipation against the bed and banks of a river) as high as  $4000 \text{ W m}^{-2}$ , and extremely high erosion rates largely from landsliding (Wang et al., 2014). Within the 5 km deep Gorge there appears to be coupling through a set of positive feedbacks between high rates of erosion, crustal deformation, metamorphism, and rapid exhumation although the link with metamorphism is contested (Whipple, 2014), some of the feedbacks are uncertain (King et al., 2016), and precipitation appears to have only a small effect on the spatial pattern of denudation (according to Finnegan et al., 2008). Salvi et al. (2017) cite Chinese research that suggests funnelling of moist monsoon air along the Siang River into the Gorge producing localized heavy precipitation. Landslide erosion rates are correlated with exhumation rates and stream power, and within the 2000 km<sup>2</sup> area of high exhumation rates in the Gorge the rate of sediment production by landsliding was between  $10.6$  and  $31.8 \times 10^6$  t yr<sup>-1</sup> for the 30-year period prior to 1974 (Larsen and Montgomery, 2012). In the area of lower exhumation rates the landslide erosion rates were lower than in the area of high exhumation by factors between 4 and 5. The correlation between landslide erosion rates and stream power shows that channel incision and lateral erosion of hillslope toes triggers landslides (Yang et al., 2021), the best documented case of toe erosion in the Gorge being the 2000 flood from a landslide lake outburst flood (LLOF) on Zhamu Creek in Tibet (Fig. 8) (Delaney and Evans, 2015) which caused landslide erosion equivalent to  $\sim 75\%$  of the total landslide erosion over a 33 year period in the zone of high exhumation (Larsen and Montgomery, 2012). Channel incision may also increase the angle of adjoining hillslopes and cause more landslides, but channel incision is spatially and temporally variable in the massif as it is minimal where alluvium accumulates, for example in the area of alluviation after the 2000 flood and may also be limited by the absence of abrasive sediment particles. That said, Finnegan et al. (2008) conclude that landslides amplify river incision in the Gorge by providing abrasive tools

from sediment particles where there is high stream power and therefore little alluviation, but incision will be limited where stream power is low and alluviation common. Where incision is high there will be a positive feedback to adjacent hillslope angles and landslide erosion rate. Ouimet et al. (2007) provided a longer-term perspective on these processes.

As shown by Larsen and Montgomery (2012), LLOFs are an extremely efficient agent of both erosion and sediment transport in the Gorge and into the Brahmaputra River. Glacial lake Outburst Floods (GLOFs) from the Tibetan Plateau also produce megafloods, and there also appear to be polygenetic floods produced by combinations of LLOFs and GLOFs. LLOFs mainly appear to be a consequence of rainfall on steep terrain, while GLOFs are a result of glacier advances that dam valleys and create lakes that burst. Dasgupta and Mukhopadadhyay (2014) added the suggestion that earthquakes can also cause landslides that lead to LLOFs, and they analysed the 2000 LLOF showing a spatial coincidence between a swarm of earthquakes and the landslide area. Petley (<https://blogs.agu.org/landslideblog/2018/01/02/yarlung-tsangpo-1/>; accessed 11th August 2021) drew attention to three large landslide dams on the Yarlung-Tsangpo River that were triggered by a magnitude 6.4 earthquake (<http://www.gdacs.org/report.aspx?eventtype=EQ&eventid=1126722>; accessed 11th August 2021) in Tibet. The lakes are however much smaller than that which produced the LLOF in 2000. Many small LLOFs appear to occur on the Plateau that don't reach the syntaxis (Chen et al., 2020a, 2020b).

The documentation of megafloods that have travelled down the Gorge is based on Montgomery et al. (2004), Chen et al. (2008), Lang et al. (2013), Turzewski et al. (2014), Dasgupta and Mukhopadadhyay (2014), Liu et al. (2015), Delaney and Evans (2015), Srivastava et al. (2017), Panda et al. (2020). Megafloods are known to have occurred as follows: 2000 CE, 1900 CE, possibly one flood between 1900 and 2000 CE, two between 1760 and 300 CE, one about  $1.3 \times 10^3$  years BP, five between  $2.4$  and  $5 \times 10^3$  years BP, one between  $6$  and  $8 \times 10^3$  years BP, 18 between  $18$  and  $27 \times 10^3$  years BP, one earlier than  $32 \times 10^3$  years BP, one earlier than  $50 \times 10^3$  years BP. Montgomery et al. (2004) dated megafloods to about  $9 \times 10^3$  years BP and about  $1.5 \times 10^3$  years BP, but Chen et al. (2008) found that they were much older. Srivastava et al. (2017) drew attention to the coincidence of floods with wet periods between  $23.3$  and  $17 \times 10^3$  years BP and  $8$  and  $6 \times 10^3$  years BP, based on the speleothem (carbonate deposits in caves) palaeoclimatic record of Dutt et al. (2015) from Meghalaya. Importantly for the purposes of this paper, none of the authors mention human agency among the causes of megafloods, such as deforestation leading to landslides and LLOFs, perhaps because the power of nature is believed to overshadow human agency. Within the past 1300 years, a time when the climate was like that of the present (Chen et al., 2020a, 2020b), there have been six megafloods into the upper Brahmaputra, with an average frequency of one every 220 years. The same phenomena occur in the Lohit and Dibang catchments of the Mishmi Hills (C. Sheth, [https://www.conser vationindia.org/wp-content/files\\_mf/Sheth-2020-Dibang-Natural-Hazards-full-report.pdf](https://www.conser vationindia.org/wp-content/files_mf/Sheth-2020-Dibang-Natural-Hazards-full-report.pdf); accessed 31 August 2021).

### 6.3. The banks of the Brahmaputra and channel relocations

As already noted, the Brahmaputra has been widening over most of its length by bank erosion (Lahiri and Sinha, 2012; Sarma and Acharjee, 2018; and references therein) as it shallowed. Between 1912 and 2009 the average width change was 3060 m between Kobo and Dhubri (Sarma and Acharjee, 2018). Adopting an average riverbank height of 2-3 m and a bulk density for riverbank material of 1.5, the input to the river from channel widening was between  $55$  and  $83 \times 10^6$  t yr<sup>-1</sup>, or between 8 and 13% of the annual average input to the river from the tributaries of  $658 \times 10^6$  t yr<sup>-1</sup>, a figure that seems to be too large and needs a more rigorous analysis. Lupker et al. (2017; and Lupker pers. comm., 2019) cannot distinguish this amount given the uncertainties in their estimates.

Relocations of rivers, such as the shift of the Lohit after the exceptional flood of 1998 and changes to the Dibang River (C. Sheth, [https://www.conservationindia.org/wp-content/files\\_mf/Sheth-2020-Dibang-Natural-Hazards-full-report.pdf](https://www.conservationindia.org/wp-content/files_mf/Sheth-2020-Dibang-Natural-Hazards-full-report.pdf); accessed 31 August 2021) flush out large quantities of sediment. But there are no estimates of the quantities involved, and some is being trapped in rivers that have low transport capacity, such as the Kundil River after it received more sediment from a new tributary because of the flood in 1998 (Borgohain et al., 2017).

### 6.4. The tributaries

Erosion processes and triggers in the tributary catchments downstream of the syntaxis include landslides caused by earthquakes, rainfall, weathering, and road construction; channel incision and relocation; riverbank erosion; LLOFs and GLOFs; and sheet and rill erosion. Each will now be considered.

#### 6.4.1. Landslides and related phenomena

As already noted, from results reported by Mathur (1953) some  $7.5 \times 10^{10}$  t of landslide sediment was produced by the 1950 earthquake, although this is a rough estimate according to Marc et al. (2016) who, using a different and more physically sound method, estimated the volume at  $2 \times 10^9$  t over an area of  $60 \times 10^3$  km<sup>2</sup> (Marc et al., 2017). An unknown fraction of this mass reached rivers such as the Lohit to raise the bed of the Brahmaputra and move downstream into Bangladesh, possibly as a damped oscillation. Other great earthquakes have occurred, probably on the Himalayan Frontal Thrust (HFT) (which defines the southernmost margin of the orogen along the entire Himalayan arc; Srivastava et al., 2017), although Drukpa et al. (2017) other faults may be involved, particularly the Main Himalayan Thrust and the Topographic Frontal Thrust. Great to large earthquakes have been documented from the Himalayan part of the Brahmaputra valley, one of which occurred in 1255 CE (Mishra et al., 2016a, 2016b) and others in 1897 CE (on the edge of the Shillong Plateau), 1947 CE, 1713 CE, 1713CE, and 1697 CE (Priyanka et al., 2017), two on the HFT in Bhutan, one after  $1570 \pm 80$  CE and another after  $1150 \pm 100$  CE (Berthet et al., 2014). Le Roux-Mallouf et al. (2016), also in Bhutan, found evidence for either a series of great earthquakes between 1025 and 1520 CE or a single giant earthquake between 1090 and 1145 CE that may have had a magnitude of 8.7–9.1. As an example of the likely effect of these earthquakes, in the Teesta River catchment, using the global empirical relationship between earthquake magnitude and landslide volume of Malamud et al. (2004),

the earthquake in about 1100 CE with a magnitude between 8.7 and 9.1 (Berthet et al., 2014) would have produced between 33 and  $122 \times 10^{10}$  t of landslide sediment, much of which could have reached either the Mo Chhu (also known as the Sankosh River) and/or the Drangme Chhu (or Manas River) and eventually the Brahmaputra. A later earthquake probably in 1714 CE (Hétenyi et al., 2016) with a magnitude of about 8 also would have produced about  $3 \times 10^6$  t of sediment, some of which would have reached the same rivers as the earlier earthquake. Better estimates of these masses and the areas over which they were generated could be produced by using the method of Marc et al. (2016) and Marc et al. (2017), but this would require a separate research project. Whatever the amount of sediment produced by this process, and assuming that the channel bed waves in the rivers downstream of the landslide areas relax back to a background level in less than a century (given the evidence presented earlier from the Teesta River and that elsewhere in the Himalaya this takes much less than 300 years - Cook et al., 2018; or perhaps only a few decades – Tanyas et al., 2021), the transport rate estimated using  $^{10}\text{Be}$  will include both the background rate and the perturbation from earthquakes in a multi-century or millennial average.

With a view to the future Mishra et al. (2016a, 2016b) concluded that, on the Himalayan front of the Brahmaputra valley, to reduce to zero the estimated slip deficit requires earthquakes of magnitude 7.7 to 8.6. They also conclude that magnitude 9 earthquakes are possible on the Himalayan arc (also see Coudurier Curveur et al., 2016). Tectonic strain is accumulating in the Himalaya and the Indo-Burman ranges, but not in the Shillong Plateau where the bounding faults appear to be locked (Jade et al., 2007). Two large earthquakes with epicentres on the Brahmaputra plain occurred in 1548 CE, near the southern margin of the plain, and in 1697 CE near Sadiya (Fig. 2) close to the junction of the Lohit and Brahmaputra rivers (Reddy et al., 2009), the former of which would not have produced large amounts of sediment given its location but that near Sadiya may have produced many landslides, judging from a court chronicle of 1697 CE (Ragendran et al., 2004).

Additional evidence of active tectonics along the Himalayan front, in the form of deformed fans, uplifted river terraces, antecedent gorges, and triangular faceted slopes, comes from Misra (2007), Agarwal et al. (2009), Luirei et al. (2012), and Bhakuni et al. (2013). Srivastava et al. (2008) demonstrated uplift within the past  $3 \times 10^3$  years on the Siang River and Srivastava and Mishra (2008) estimated uplift at an average rate of 7.5 mm yr<sup>-1</sup> over the past  $14 \times 10^3$  years on the Kameng River. Berthet et al. (2014) estimated an uplift rate on the HFT for about the last  $6 \times 10^3$  years of about 8 mm yr<sup>-1</sup>. Not only are there earthquakes along the Himalayan front, which generate large quantities of landslide sediment, but also uplift enables river incision that generates sediment and steepens adjacent hillslopes that erode faster than gentle slopes, often by landsliding.

Uplift, steep slopes and landsliding are complimented by other processes of erosion. In the Teesta River catchment, the highest erosion rates are around the Main Central Thrust Zone (MCTZ) and in the glaciated area further north, according to the research of Abrahami et al. (2016) based on  $^{10}\text{Be}$ . Higher rates of erosion in the MCTZ are probably related to active uplift and landsliding in this area of high relief where annual rainfall is between 2 and 3 m, although for the entire study area there is no statistical relationship between erosion and rainfall. In the northern area high erosion rates occur near the former extent of glaciers where there are also the steepest channel gradients, suggesting that

readjustment of the denudation system is occurring after the retreat of glaciers from their limit at the Last Glacial Maximum that involves channel gradient changes, landslides, and paraglacial sediment production; i.e., erosion and transport of sediment left as moraines after glacial retreat. Portenga et al. (2015) showed that in small catchments high erosion rates also occur near the glaciated part of Bhutan and where rainfall is highest, and erosion is lowest where rainfall is low.

Landslides occur along active fault scarps, between the Siang and Dibang river valleys (Luirei et al., 2012), in the Lohit and Dibang valleys (Misra, 2007), along the Kamla River (Bhakuni et al., 2013), and in the Kimin-Ziro area of the Lower Subansiri District (Agarwal et al., 2009), particularly on steep slopes where the rocks are shattered (Luirei and Bhakuni, 2008). Landslides also occur on the walls of antecedent gorges. Rawat and Joshi (2012), in the Igo River catchment in the West Siang District of Arunachal Pradesh, found that rock type and structure, slope and relief are much more important explanatory variables of landslide location than land use. In Nagaland in the Indo-Burman ranges Yhosu and Krishnaiah (2017) showed that building construction on weak rocks produces hazardous landslides. According to Pandey et al. (2008) faults (and associated locally steep slopes and ground shaking) are the most important cause of landslides in the Dikrong valley, followed by (in order of decreasing importance) rock type, land use, lineaments (that may be infrequently active faults), slope, relief, and drainage density. This is not a surprising result as Mishra et al. (2016a, 2016b) provided evidence in this catchment of active tectonics in the form of thrusts and anticlinal growth (Agarwal et al., 2009).

Much less appears to be known in the Indo-Burman Ranges (Fig. 3) about active tectonics and sediment generation. Seismicity is strongly associated with ongoing subduction of the Indian Plate beneath the Burma Plate (a micro-plate within the Eurasian Plate) (Bahuguna and Sil, 2018). Aier et al. (2011) provided detailed evidence for active tectonics in Nagaland in the form of truncation of river terraces, strath terraces, tilting of fans and river terraces, lateral displacement of rivers, and thrusting of Miocene rocks over Quaternary sediments of the Brahmaputra plain. One of the major tectonic features of this area is the Disang Thrust along which can be found many landslides, the occurrence of which is exacerbated by road construction. Once again, there is evidence for tectonics playing a role in generating sediment that in this case could reach the Brahmaputra down the Diphu and Dzuza rivers. There are no glaciers in these ranges, and therefore GLOFs cannot occur, and LLOFs have not been reported.

As will be shown later, there is evidence of enhanced erosion by deforestation, but no knowledge of the amount of sediment that reaches streams as a result. It is important to note that because the  $^{10}\text{Be}$ -derived denudation rates are averaged over centuries to millennia they usually cannot be used for detection of the effects of recent land cover change, unless they are compared with estimates from recent times which also include solute losses to be consistent with the results from  $^{10}\text{Be}$ , although see Rosenkranz et al. (2018) for a more detailed argument for the Shillong Plateau. Also, the  $^{10}\text{Be}$ -based denudation rates are likely to be underestimates if derived in small catchments. The catchments sampled in Sikkim by Abrahimi et al. (2016) range in size from 0.82 to 8033 km<sup>2</sup> in area, with a range of averaging times of 8600 to 113 years. For the research in Bhutan by Portenga et al. (2015) the range of catchment areas is  $2\text{-}10 \times 10^3$  km<sup>2</sup> and the mean of the averaging times is about 700 years. Assuming that landslides are important if not the dominant

process of denudation in these high mountain catchments, from Fig. 8 of Marc et al. (2018a, 2018b) the time required for averaging landslide temporal variability is between 200 and 106 years, implying that most of the results from these two studies will be underestimates of denudation rates. Le Roux-Mallouf et al. (2015) avoided small catchments, but almost all their sampled catchments are <100km<sup>2</sup> in area and the denudation rate averaging times are less than those needed to take account of the variability of landslides for the sampled catchments, although the extent to which this is a problem depends upon landslide frequency. The results of Lupker et al. (2017) and Singh and France-Lanord (2002) are probably not underestimates who mostly sampled large catchments and denudation rate averaging times from 300 to  $3.2 \times 10^3$  years. The problem of underestimation, however, applies to the work of Finnegan et al. (2008) in the syntaxis. And the situation is worse for denudation rate estimates based on measurements of sediment transport where, only in catchments as large as 105km<sup>2</sup>, can the variability of landslides be accounted for, meaning that Goswami's (1985) results are likely to be underestimates. While there is general understanding of the relationships between rainfall-induced landslides, storms, and total rainfall, and that these landslides occur preferentially on intermediate slopes rather than on the steepest slopes (which is the case for earthquake-induced landslides) (Marc et al., 2018a, 2018b), the absence of an inventory of landslides triggered by rainfall in the Brahmaputra catchment makes it impossible to judge the quantitative significance of this erosion process for the sediment budgets of tributary catchments.

That said, the study by Starkel and Basu (2000) is a very detailed account of the many landslides triggered by intense and prolonged rainfall in 1968 in the Teesta catchment. (Figure s 4 and 6). Large numbers of landslides were caused at a rate twenty times higher on deforested hillslopes by comparison with forested slopes. Channel sedimentation followed, at least 15 km from the mountain front. In catchments 5-20 km<sup>2</sup> in area debris flows deposited sediment up to 10 m deep and as sediment delivery fell channels were incised by up to 7 m. At Teesta Bazaar (Fig. 6), upstream of the mountain front, the river widened after the depositional event, analogous to what has happened in the Brahmaputra after 1950, and the riverbed elevation rose by 5-6 m and since 1974 had fallen. By 1984 hillslopes stripped of vegetation by landslides caused by slope undercutting by the high flows in 1968 had become revegetated and the longitudinal profiles of channels were becoming smoother, suggesting a return to the pre-1968 state. Within the tributary catchments there appears to be little known about road-induced sediment production for which there are descriptions (e.g., Luirei and Bhakuni, 2008) but only one known estimate of the amount by Starkel and Basu (2000) who showed that over a length of 6.5 km of roads  $17 \times 10^3$  m<sup>3</sup> (about  $2.6 \times 10^3$  m<sup>3</sup> km<sup>-1</sup>) was mobilized during the 1968 rainfall event in the Teesta catchment.

#### 6.4.2. LLOFs and GLOFs

Landslides from the 1950 earthquake blocked several of the major tributaries forming lakes and then LLOFs (Luirei and Bhakuni, 2008; Kingdon-Ward, 1955). As noted earlier, the bursts of high velocity water move substantial amounts of sediment downstream, scour riverbanks and widen rivers, and undercut adjoining hillslopes and cause land-



slides. All these processes inject more sediment into downstream channels causing aggradation and a new sediment wave. GLOFs produce similar results, but there is in the Brahmaputra catchment a focus on the hydrology of GLOFs rather than on sediment production and transport (Panda et al., 2014; Gurung et al., 2017). In the comparison of a GLOF and monsoon sediment transport, Cook et al. (2018) concentrated on channel scour and undercutting of adjoining hillslopes rather than on aggradation. Cook et al. (2018) suggest that GLOFs may dominate fluvial erosion in the Himalaya, but the lower elevation parts of the Himalaya are not susceptible to GLOFs, as there are no glaciers, but there are LLOFs. However, the combination of GLOFs and LLOFs may dominate fluvial erosion and sediment transport from source areas. This possibility, when combined with the episodic nature of great earthquakes and landslides of all origins, suggests that much of the production of sediment is episodic and any estimates of the respective importance of different sources must include documentation of temporal variability.

#### 6.4.3. Sheet and rill erosion

Sheet and rill erosion of hillslopes should also be considered. The research by Dabral et al. (2008), Pandey et al. (2009), and Rawat et al. (2013) in the Dikrong River catchment (Fig. 4) used erosion plots, the Universal Soil Loss Equation, and the Morgan-Morgan Finney model to estimate soil loss under different vegetation covers. For the purposes of this paper the work of Pandey et al. (2009) is the most useful as it estimated soil loss over the entire catchment. Most soil loss is on steep slopes with sparse vegetation, and in jhum cultivation (slash and burn) or abandoned jhum cultivation, although they also implicate high rainfall and fragile soils and rocks. A similar result was found in the Kale River Catchment in the Ziro area of the Lower Subansiri District in Arunachal Pradesh (Riba and Joshi, 2014). In the Nirjuli sub-catchment of the Dikrong catchment Rawat et al. (2013) showed that their barren (grassed) field plot lost 2.7 times the amount of soil as the forested plot, while the jhum plot lost 6.2 times that of the forested plot. Pandey et al. (2009) also showed that average annual soil loss in the Dikrong catchment increases with annual rainfall, and analysis of their data shows that the relationship is strongly linear with a value of  $r^2$  of 0.9016 ( $p < 0.0001$ ) suggesting that as rainfall increases with future atmospheric warming (Darby et al., 2015) soil loss will increase if further soil conservation measures are not taken.

While valuable, the studies of soil loss from sheet and rill erosion provide no information about the amount of sediment derived from these processes that reaches rivers. And despite there being a lot of information about sediment sources in the Dikrong River catchment in particular, the proportionate contribution of each to river sediments is unknown. That is, do landslides dominate, and what is the contribution from channel incision and sheet and rill erosion?

#### 6.4.4. Channel incision and relocations

Incision rates are known at a few locations on the Himalayan front, but there do not appear to be estimates of sediment excavation rates by this process. Channel relocations have been

mapped by several authors, but there do not appear to be any calculations of the amount of sediment moved downstream by this mechanism. With measured riverbank heights, estimates could be made of the amount of sediment produced. This would not however provide estimates of the transport of this sediment downstream or its storage.

## 7. Spatial patterns of sediment yield in the tributaries

Profoundly important criticisms of hydrologic research and that focused on erosion and sediment transport in the Himalaya are: local studies concentrate on physical variables (such as rainfall, runoff, and landslides); those at regional and continental scales focus on natural resource issues with poor definition of relevant physical variables, and spatial and temporal scales; and many studies have tried to scale up to regions from local scales (Gamble and Meentemeyer, 1996). The last of these criticisms is particularly important as it takes no account of the processes and rates of sediment production and storage that are scale dependent. Therefore, explicit account should be taken of spatial variation within tributary catchments of sediment sources, especially for management purposes.

The account provided earlier of the results from Lupker et al. (2017) supplies a spatially explicit picture of sediment sources in the Brahma-putra catchment represented by sediment transport rates in the rivers that complements the tectono-geomorphic zonation. Further analysis of their data shows that for the rivers with catchments <122,000 km<sup>2</sup> in area (Dibang, Lohit, Burhi Dibang, Subansiri, Kameng, Manas, Tsang Chhu, and Teesta; Fig. 4) there is a direct linear relationship between catchment area and specific sediment yields (t km<sup>2</sup> yr<sup>-1</sup>) with  $r^2$  of 0.616 and  $p = 0.0211$ . The same pattern was found by Portenga et al. (2015) in the PunaTsang Chhu catchment of Bhutan (Fig. 4). From a global synthesis, but with emphasis on catchments in the Eurasian temperate zone, Dedkov (2004) concluded that increasing specific sediment yield with catchment area, the so-called direct pattern in contrast with the inverse pattern where yield declines with area, occurs where human impact is slight, particularly where the area of cultivation is small. He further concluded that where there is a dense cover of vegetation both sheet and gully erosion is limited and most sediment derives from erosion of river channels. The same conclusion was reached by Birkinshaw and Bathurst (2006) from a modelling study. But these conclusions may not apply in the mountains of the Brahma-putra catchment where channel erosion is probably a small fraction of the total sediment production and, as in the Himalaya generally, landslides may dominate (Marc et al., 2018a, 2018b). Portenga et al. (2015) ascribe the direct relationship between catchment area and sediment transport rate in their data to rapid transport of sediment through channels with little sediment storage, a more likely explanation that should also apply to the data from the smallest catchments of Lupker et al. (2017) noting that almost all their samples for these catchments came from close to the mountain fronts. But on the Teesta River two samples, one close to the Brahmaputra, indicates that  $20 \times 10^6$  t yr<sup>-1</sup> was added to the river on the plain, pre-sumably by channel erosion, at a rate of about  $100 \times 10^3$  t km<sup>-1</sup>, assuming that the year-to-year variability in the <sup>10</sup>Be signal in the Teesta is not large. Ray (1956) reported widening of this river by riverbank erosion, consistent with the explanation of the results from the <sup>10</sup>Be results although on different timescales.

## 8. A role for deforestation?

In the Introduction a plea was made for evidence-based conclusions and decision-making. Debate about the role of deforestation in enhancing erosion and sedimentation in the Indian Himalaya has a history stretching back to the nineteenth century (e.g., Haigh, 1984; Wasson, 2008; Wasson et al., 2008), with little resolution. The claim that deforestation leads to increased erosion (uncontested) and major additions of sediment to rivers (unknown in the Brahmaputra catchment), thereby exacerbating floods in the Brahmaputra system (unknown), a recent example being from Tewari (2004) while Pandey et al. (2008) claim that *jhum* has the same effect.

In 1999 about 20% of Assam was forested and Khataniar et al. (2012) estimated a reduction of forest cover between 1999 and 2001 of 123km<sup>2</sup>, mostly enabled by access to forests provided by road construction, a well-known phenomenon globally. In the Eastern Himalaya (Sikkim and Arunachal Pradesh but excluding Bhutan) Pandit et al. (2007) documented a 7% loss of forest between 1970 and 2000 and a projected loss of 28% by 2100 if the rate to 2000 continues. In 2000 forest covered 77% of the Eastern Himalaya, taking no account of the area above the tree line, which is about 30% (Mishra et al., 2004). Although there are others, a particular hotspot of deforestation occurs in Sonitpur District of Assam where between 1994 and 2001 about 29% of forest was lost (Srivastava et al., 2002). This high loss rate is attributed to increasing population and conversion of forest to arable, illegal logging, and the increasing insurgency problem, although an explanation of the role in deforestation of this last cause is not provided. Another hotspot is the surface of the Shillong Plateau (Fig. 3) where erosion rates based on <sup>10</sup>Be and <sup>137</sup>Cs are high and of the same magnitude because of both deforestation and agriculture (particularly *bun*, a modified form of *jhum*) in the view of Rosenkranz et al. (2018) and Prokop and Poreba (2012). Even though erosion rates on the forested incised margins of the Plateau are much lower, this edifice provides about 11% of the Brahmaputra sand upstream of the junction with the Teesta River (Garzanti et al., 2004).

Deforestation is therefore a real phenomenon in the Brahmaputra catchment and Wasson (2008) summarized then available information from other parts of the Himalaya that demonstrate a link between deforestation, enhanced erosion, and channel aggradation, particularly in the Alaknanda River catchment and Darjeeling Himalaya in the Teesta River catchment. Such studies are yet to be done widely in the Brahmaputra system.

A guide can nonetheless be provided. If up to 40% of the sediment flux in the Brahmaputra downstream of the syntaxis comes from the Himalaya (Table 1), then deforestation and *jhum* are likely to affect only a fraction of the 20% of the Himalaya which is occupied by the LH and the few percent of the area of the Siwaliks (based on a map in Garzanti et al., 2004). This does not however provide quantification of either the amount of erosion or sediment delivery to streams. The expansion of towns and villages may also play a role in deforestation. Unfortunately, we could find no data from which this could be documented.

## 9. Discussion and conclusions

The best current knowledge shows that about 45% of the modern sediment in the Brahmaputra River comes from the syntaxis, with additional sediment from downstream tributaries with less than 1% from the Indo-Burman Ranges, 10% from the Mishmi Hills, and 40% from the Himalaya. The Siwalik foothills are neglected in this assessment and may be a significant sediment source given the results from elsewhere in the Himalaya (Jain et al., 2022). A summary of the best estimates of contributions to the Brahmaputra where it enters Bangladesh along with the major processes of sediment production is presented in Table 2 and Fig. 9. The Mishmi Hills and Himalaya have the largest number of different processes and therefore will be the most difficult to manage for reducing sediment production. They will also require the greatest effort to increase understanding of sediment sources. Also, there are significant differences between the tributary catchments in the proportions from the Tethyan Himalaya (TH), High Himalaya (HH) and Lesser Himalaya (LH). For example, most of the sediment in the Teesta River is from the LH while the Subansiri receives sediment from all the terrains, but again the role of the Siwaliks is unknown in both cases. Within each of these zones there are likely to be different sources, in some cases more landslides than elsewhere for example. But before making that conclusion the individual sources need to be identified. This is the major knowledge gap. That said, possible management interventions for the major sediment production processes will now be reviewed as an input to future research and decisions.

### 9.1. Landslides

Those caused by great earthquakes probably cannot be managed because, as shown by the startling photographs by Kingdon-Ward (1955), even the well-vegetated hillslopes in the area affected by the 1950 earthquake failed. And the hillslopes along the rivers scoured by LLOFs following the earthquake generated landslides. Limiting landslides caused by weathering along the joints and zones of weakness in bedrock is also unlikely as these zones are difficult to detect and even harder to mitigate. Landslides caused by lesser earthquakes and rainfall may be limited by maintaining vegetation on tectonically active fault scarps and downslope of scarps where landslide runout could add sediment directly to rivers.

Roads cut along steep hillslopes in the Himalaya are notoriously susceptible to failure and landsliding during earthquakes and sustained rainfall. Slopes destabilized by road construction also fail. And the excavation of the space for roads generates sediment that is usually disposed of in rivers. Solving these problems in the Himalayan terrain is challenging but is worthy of greater attention.

### 9.2. GLOFs and LLOFs

GLOFs can be anticipated by mapping the most dangerous lakes, then draining them before they are close to failure, but not without considerable cost and difficulty. GLOFs may be responsible for the mobilization of old glacial deposits in the high mountains, but in the areas of former glaciation the natural process of river incision and landsliding also appear to

be at work, processes that may be exacerbated by high altitude grazing which can be managed.

Landslide lakes that fill slowly can be identified and drained but managing lakes that form either during or in the immediate aftermath of massive landsliding by whatever cause is difficult as their formation and bursting occurs too quickly under very dangerous circumstances for people who may wish to assist.

### 9.3. Riverbank erosion and channel relocations

Each of the management interventions just described may be individually of value to reduce sediment fluxes, but the respective contributions of each to the total sediment loads in the Brahmaputra and its tributaries are unknown. The standard approach to estimating these contributions is to construct a sediment budget (Reid and Dunne, 2016) by measuring rates of sediment production, transport, storage, and output from a catchment. This would be a very difficult, time-consuming and resource intensive approach in the Brahmaputra catchment, and another approach is therefore needed. The only catchment-wide attempt at a partial sediment budget is by Bhattacharya et al. (2018) using the SWAT model, but they could not test their results because of a lack of erosion rate and sediment yield data.

The most efficacious alternative approach relies upon geochemical tracers, building on previous studies that have used this approach (e.g., Lupker et al., 2017; Singh and France-Lanord, 2002) and should be focused on the Himalayan tributary catchments downstream of the syntaxis. The first question to be answered is: What is the proportion of sediment derived from the TH, HH, LH, and the Siwaliks in the Himalayan catchments? Once this is answered, the focus can turn to the key processes of sediment generation in each catchment and management opportunities. It is suggested that a study should be modularized, the first module of which would be a pilot study to determine both the effectiveness of the approach and, if appropriate, plan the next module. For the first module the following tasks will be necessary.

Task 1. Determine the proportions of sediment derived from the TH, HH, LH and Siwaliks in the major tributaries emanating from the Himalaya. This can be accomplished by measuring Sr and Nd isotopes for estimates of modern sediment sources, and  $^{10}\text{Be}$  for longer-term sources (in catchments large enough to capture landslide variability) in samples from the headwaters to the mountain front. Two catchments should be selected for a pilot study (although it is known to be effective; Wasson et al., 2008; and see Froehlich and Walling, 2006), one of which could be the Dikrong, not because it is likely to be a major sediment source but because much is known about it.

Task 2. . Because of the episodic nature of sediment production in the mountains, from earthquakes, GLOFs, LLOFs, and rainfall events, geochemical tracers should also be measured in sedimentary archives, such as in-channel benches, that are centuries to millennia old to be dated by Optically Stimulated Luminescence. This approach has already been successfully applied in the Himalaya (Wasson et al., 2008).

Task 3. Surface soil input to rivers, particularly from areas of cultivation and jhum, can be estimated by measuring the fallout radionuclides  $^{137}\text{Cs}$  and  $^{210}\text{Pb}(\text{ex})$ , and Pu isotopes, all

which label surface soils. By difference from the calculated surface soil proportion, subsoil inputs from streambanks, gullies and landslides can also be estimated. Samples would be taken of mud along the rivers at the same locations as the samples for other tracers, paying close attention to areas where deforestation, settled agriculture and jhum occur. Samples would also be needed from undisturbed low gradient hilltops to provide input values to the catchments of the fallout nuclides, from footslopes to approximate quantities that leave the bulk of the hillslopes, and from the river mud to estimate the proportion of sediment coming from soil surfaces and from subsoils mobilized by landslides for example. Sampling would be in the same pilot catchments used for Tasks 1 and 2.

#### Author contributions

All three authors conceptualized the project. RJW acquired funding, organized statistical analysis, and wrote the first draft. SA and RR added material, edited the drafts, and checked the submitted version.

#### Declaration of Competing Interest

There are no competing interests.

#### Acknowledgements

This paper was inspired by Deep Pagu and Rajesh Baruah of the Assam Water Resources Department in Dibrugarh who told us that they were faced by a sediment problem in the Brahmaputra rather than a water problem, meaning that sedimentation was exacerbating floods. The National University of Singapore provided financial support, and they played no part in the study design, data collection, analysis and interpretation of data, the writing or the decision to publish. Officers of the Department of Water Resources of Assam, Maarten Lupker, and Eva Enkelmann provided advice. Priya Bansal assisted with statistical analysis. Two anonymous reviewers and the handling editor Dr. Christopher Fielding provided advice that has improved the paper.

## References

- Abrahami, R., van de Beek, P., Huyghe, P., Hardwick, E., Carcaillet, J., 2016. Decoupling of long-term exhumation and short-term erosion rates in the Sikkim Himalaya. *Earth Planet. Sci. Lett.* 433, 76–88.
- Agarwal, K.K., Bali, R., Kumar, M.G., Srivastava, P., Singh, P.V., 2009. Active tectonics in and around Kimin-Ziro area, lower Subansiri District, Arunachal Pradesh, NE India. *Z. Geomorphol.* 53 (1), 109–120.
- Aier, I., Luirei, K., Bhakuni, S.S., Thong, G.T., Kothyari, G.C., 2011. Geomorphic Evolution of Medziphema Intermontane Basin and Quaternary Deformation in the Schuppen Belt, Nagaland, NE India.
- Alam, S., Ali, Md.M., Rahaman, Z., Islam, Z., 2021. Multi-model ensemble projection of mean and extreme streamflow of Brahmaputra River Basin under the impact of climate change. *J. Water Clim. Change* 12, 5. <https://doi.org/10.2166/wcc.2021.286>.
- Angelier, J., Baruah, S., 2009. Seismotectonics in Northeast India: a stress analysis of focal mechanism solutions of earthquakes and its kinematic implications. *Geophys. J. Int.* 178, 303–326.
- Bahuguna, A., Sil, A., 2018. Comprehensive Seismicity, Seismic Sources and Seismic Hazard. <https://doi.org/10.1080/13632469.2018.1453405>.
- Berthet, T., Ritz, J.-F., Ferry, M., Pelgay, P., Cattin, R., Drukpa, D., Braucher, R., Hetényi, 2014. Active tectonics of the eastern Himalaya: new constraints from the first tectonic geomorphology study in southern Bhutan. *Geology* 45 (5), 427–430.
- Bhakuni, S.S., Luirei, K., Kothyari, G.C.H., 2013. Neotectonic Fault in the middle part of Lesser Himalaya, Arunachal Pradesh: a study based on structural and morphotectonic analyses. *Himal. Geol.* 34 (1), 57–64.
- Bhattacharya, B., Conway, C., Solomatine, D., Masih, I., Craven, J., Mazumder, L.C., Mazzoleni, M., Ugay, R., van Andel, S.J., Shresta, S., 2018. Hydrological and erosion modelling of the Brahmaputra basin using global datasets. In: In Loggia, G. La., Freni, G., Puleo, V., Marchis, M. De (eds.). *HIC 2018 13th International Conference on Hydroinformatics (EPIc Series in Engineering, 3)*, pp. 245–251.
- Birkinshaw, S.J., Bathurst, J.C., 2006. Model study of the relationship between sediment yield and river basin area. *Earth Surf. Process. Landf.* 31 (6), 750–761.
- Borgohain, S., Das, J., Saraf, A.K., Singh, G., Baral, S.S., 2017. Structural controls on topography and river morphodynamics in Upper Assam Valley, India. *Geodin. Acta* 29 (1), 62–69. <https://doi.org/10.1080/09853111.2017.1313090>.
- Bracciali, L., Parrish, R.R., Najman, Y., Syme, A., Carter, A., Wijbrans, J.R., 2016. Plio-Pleistocene exhumation of the eastern Himalayan syntaxis and its domal ‘pop-up’. *Earth-Sci. Rev.* 160, 350–385.

Burgess, W.P., Yin, A., Dubey, C.S., Shen, Z.-K., Kelty, T.K., 2012. Holocene shortening across the Main Frontal Thrust zone in the eastern Himalaya. *Earth Planet. Sci. Lett.* 357-358, 152–167.

Chen, Y., Huang, S., Lin, Y., Liu, J., Chung, L., Lai, K., Zhao, S., Yin, G., Cao, Z., 2008. Holocene megafloods? Stories of the lacustrine strata along the Nyang River, Tibet. In: American Geophysical Union, Fall Meeting abstract PP21A-1404.

Chen, Y., Syvitski, J.P.M., Gao, S., Overeem, I., Kettner, A.J., 2012. Socio-economic Impacts on Flooding: a 4000-year history of the Yellow River, China. *Ambio* 41, 682–698.

Chen, Y., Overeem, I., Kettner, A.J., Gao, S., Syvitski, J.P.M., Wang, Y., 2018. Quantifying sediment storage on the floodplains outside levees along the lower Yellow River during the years 1580-1849. *Earth Surf. Process. Landf.* 44, 581–594.

Chen, F., Zhang, J., Liu, J., Cao, X., Hou, J., Zhu, L., Xu, X., Liu, X., Wang, M., Wu, D.,

Huang, L., Zeng, T., Zhang, S., Huang, W., Zhang, X., Yang, K., 2020a. Climate change, vegetation history, and landscape responses on the Tibetan Plateau during the Holocene: a comprehensive review. *Quat. Sci. Rev.* 243 (1064), 44.

Chen, C., Zhang, L., Xiao, T., He, J., 2020b. Barrier lake bursting and flood routing in the YarlungTsangpo Grand Canyon in October 2018. *J. Hydrol.* 583, 124603.

Cina, S.A., Yin, A., Grove, M., Dubey, C.S., Shukla, D.P., Lovera, O.M., Kelty, T.K., Gehrels, G.E., Foster, D.A., 2009. Gangdese arc detritus within the eastern

Himalayan Neogene foreland basin: Implications for the Neogene evolution of the Yalu-Brahmaputra River system. *Earth Planet. Sci. Lett.* 285, 150–162.

Cook, K.L., Andermann, C., Gimbert, F., Adhikari, B.R., Hovius, N., 2018. Glacial lake outburst floods as drivers of fluvial erosion in the Himalaya. *Science* 362, 53–57.

Coudurier Curveur, A., Kali, E., Tapponnier, P., Karakas, Ç., Ildfonso, S.M., Woerd, J., Baruah, S.M., Choudhury, S., Okal, E., Banerjee, P., 2016. Surface rupture of the 1950 Assam earthquake: active faults and recurrence interval along the Eastern Himalayan Syntaxis. *Geophys. Res. Abstr.* 18. EGU2016-15794.

Dabral, P.P., Baithuri, N., Pandey, A., 2008. Soil erosion assessment in a Hilly Catchment of North Eastern India using USLE, GIS and remote sensing. *Water Resour. Manag.* 22, 1783–1798.



- Darby, S.E., Dunn, F.E., Nicholls, R.J., Rahman, M., Riddy, L., 2015. A first look at the influence of anthropogenic climate change on the future delivery of fluvial sediment to the Ganges-Brahmaputra-Meghna delta. *Environ. Sci. Process. Impacts* 17, 1587–1600.
- Dasgupta, S., Mukhopadadhay, B., 2014. Earthquake-Landslide-Flood nexus at the lower reaches of YigongTsangpo, Tibet: remote control for catastrophic flood in Siang, Arunachal Pradesh and Upper Assam, India. *J. Eng. Geol.* 39 (1), 177–190.
- Dedkov, A., 2004. The relationship between sediment yield and drainage basin yield. In: *Sediment Transfer through the Fluvial System (Proceedings of a Symposium held in Moscow, August 2004)*, vol. 288. IAHS Publication, pp. 197–204.
- Delaney, K.B., Evans, S.G., 2015. The 2000 Yigong (Tibetan Plateau), rockslide-dammed lake and outburst flood: Review, remote sensing analysis, and process modeling. *Geomorphology* 246, 377–393.
- Drukpa, D., Gautier, S., Cattin, R., Namgay, K., Le Moigne, N., 2017. Impact of near-surface fault geometry on secular slip rate assessment derived from uplifted river terraces: Implications for convergence accommodation across the frontal thrust in southern Central Bhutan. *Geophys. J. Int.* <https://doi.org/10.1093/gji/ggx478> ggx478. (43pp).
- Dutt, S., Gupta, A.K., Clemens, S.C., Cheng, H., Singh, R.K., Kathayat, G., Edwards, R.L., 2015. Abrupt changes in Indian summer monsoon strength during 33,800 to 5500 years B.P. *Geophys. Res. Lett.* 42, 5526–5532. <https://doi.org/10.1002/2015GL064015>.
- Enkelmann, E., Ehlers, T.A., Zeitler, P.K., Hallet, B., 2011. Denudation of the Namche Barwa Antiform, Eastern Himalaya. *Earth Planet. Sci. Lett.* 307 (s 3–4), 323–333. Finnegan, N.J., Hallett, B., Montgomery, D.R., Zeitler, P.K., Stone, J.O., Anders, A.M.,
- Liu, Y., 2008. Coupling of rock uplift and river incision in the Namche Barwa-Gyala Peri massif, Tibet. *Geol. Soc. Am. Bull.* 120 (1/2), 142–155.
- Fischer, S., Pietron, J., Thorslund, J., Jarso, J., 2017. Present to future sediment transport of the Brahmaputra River: reducing uncertainty in predictions and management. *Reg. Environ. Chang.* 17, 515–526.
- Froehlich, W., Walling, D.E., 2006. The use of  $^{137}\text{Cs}$  and  $^{210}\text{Pb}$  to investigate sediment sources and overbank sedimentation rates in the Teesta River basin, Sikkim Himalaya, India. In: *Sediment Dynamics and the Hydromorphology of Fluvial Systems (Proceedings of a Symposium held in Dundee, UK, July 2006)*, vol. 306. IAHS Publication, pp. 380–388.
- Galy, A., France-Lanord, C., 2001. Higher erosion rates in the Himalaya: Geochemical constraints on riverine fluxes. *Geology* 29, 23–26.
- Gamble, D.W., Meentemeyer, V., 1996. The role of scale in research on the Himalaya-Ganges-Brahmaputra interaction. *Mt. Res. Dev.* 16 (2), 149–155.

Garzanti, E., Vezzoli, G., Ando, S., France-Lanord, C., Singh, S.K., Foster, G., 2004. Sand petrology and focused erosion in collision orogens: the Brahmaputra case. *Earth Planet. Sci. Lett.* 220, 157–174.

Gerignani, L., Beek, P.A., Braun, J., Najman, Y., Bernet, M., Garzanti, E., Wijbrans, J.R., 2018. Downstream evolution of the thermochronologic age signal in the Brahmaputra catchment (eastern Himalaya): Implications for the detrital record of erosion. *Earth Planet. Sci. Lett.* 499, 48–61.

Ghosh, S., Dutta, S., 2011. Impact of Climate and Land Use Changes on the Flood Vulnerability of the Brahmaputra Basin. *Geospatial World Forum*, 18–21 January 2011, Hyderabad paper number: PN-364.

Goswami, D.C., 1985. Brahmaputra river, Assam, India: basin degradation and channel aggradation. *Water Resour. Res.* 21, 959–978.

Gurung, D.R., Khanal, N.R., Bajracharya, S.R., Tsering, K., Joshi, S., Tshering, P., Chhetri, L.K., Lotey, Y., Penjor, T., 2017. Tsho Glacial Lake Outburst Flood (GLOF) in Bhutan: cause and impact. *Environ. Risk Assess. Remediat.* 1 (2), 7–15.

Haigh, M., 1984. Deforestation and disaster in northern India. *Land Use Policy* 1 (3), 187–198.

Hétenyi, G., Le Roux-Mallouf, R., Berthet, T., Cattin, R., Cauzzi, C., Phuntsho, K., Grolimund, R., 2016. Joint approach combining damage and paleoseismology observations constrains the 1714 A.D. Bhutan earthquake at magnitude  $8 \pm 0.5$ . *Geophys. Res. Lett.* 43, 10,695–10,702. <https://doi.org/10.1002/2016GL071033>.

Jade, S., Mukul, M., Bhattacharyya, A.K., Vijayan, M.S.M., Jaganathan, S., Kumar, A., Tiwari, R.P., Kalita, S., Sahu, S.C., Krishna, A.P., Gupta, S.S., Murthy, M.V.R.L., Gaur, V.K., 2007. Estimates of interseismic deformation in Northeast India from GPS measurements. *Earth Planet. Sci. Lett.* 263, 221–234.

Jain, V., Wasson, R.J., McCulloch, M., Kaushal, R., Singhvi, A.K., 2022. Controls on sediment provenance in the Baghmata River catchment, Central Himalaya, India. *J. Earth Syst. Sci.*

James, L.A., 2010. Secular sediment waves, channel bed waves, and legacy sediment. *Geogr. Compass* 4 (6), 576–598.

Khataniar, B., Barua, A., Talukdar, R., 2012. Dwindling forests in Assam, India: causes and remedies. *Clarion* 1 (2), 154–167.

King, G.E., Herman, F., Guralnik, B., 2016. Northward migration of the eastern Himalayan syntaxis revealed by OSL thermochronometry. *Science* 353 (6301), 800–804.

Kingdon-Ward, F., 1955. Aftermath of the Great Assam earthquake of 1950. *Geogr. J.*

121 (3), 290–303.

Lahiri, S.K., Sinha, R., 2012. Tectonic controls on the morphodynamics of the Brahmaputra River system in the upper Assam valley, India. *Geomorphology* 169–170, 74–85.

Lang, K.A., Huntington, K.W., Montgomery, D.R., 2013. Erosion of the Tsangpo Gorge by megafloods Eastern Himalaya. *Geology*. <https://doi.org/10.1130/G34693.1>, 4pp.

Larsen, I.J., Montgomery, D.R., 2012. Landslide erosion coupled to tectonics and river incision. *Nat. Geosci.* 5, 468–473.

Le Roux-Mallouf, R., Godard, V., Cattin, R., Ferry, M., Gyeltshen, J., Ritz, J.-F., Drukpa, D., Guillou, V., Arnold, M., Aumaitre, G., Bourles, D.L., Keddadouche, k.,

2015. Evidence for a wide and gently dipping Main Himalayan Thrust in western Bhutan. *Geophys. Res. Lett.* 42, 3257–3265. <https://doi.org/10.1002/2015GL063767>.

Le Roux-Mallouf, R., Ferry, M., Ritz, J.F., Berthet, T., Cattin, R., Drukpa, D., 2016. First paleoseismic evidence for great surface-rupturing earthquakes in the Bhutan Himalayas. *J. Geophys. Res. Solid Earth* 121 (10), 7271–7283.

Liang, W., Garzanti, E., Hu, X., Resentini, A., Vezzoli, G., Yao, W., 2021. Tracing erosion patterns in South Tibet: Balancing sediment supply to the YarlungTsangpo from the Himalaya versus Lhasa Block. *Basin Res.* <https://doi.org/10.1111/bre.12625>.

Liu, W., Lai, Z., Hu, K., Ge, Y., Cui, P., Zhang, X., Liu, F., 2015. Age and extent of a giant glacial-dammed lake at YarlungTsangpo gorge in the Tibetan Plateau. *Geomorphology* 246, 370–376.

Luirei, K., Bhakuni, S.S., 2008. Landslides along Frontal part of Eastern Himalaya in East Siang and lower Dibang Districts, Arunachal Pradesh, India. *J. Geol. Soc. India* 71, 321–330.

Luirei, K., Bhakuni, S.S., Srivastava, P., Suresh, N., 2012. Late Pleistocene-Holocene tectonic activities in the frontal part of NE Himalaya between Siang and Dibang river valleys, Arunachal Pradesh, India. *Z. Geomorphol.* 56 (4), 477–493.

Lupker, M., Lavé, J., France-Lanord, C., Christl, M., Bourlès, D., Carcaillet, J., Maden, C., Wieler, R., Rahman, M., Bezbaruah, D., Liu, X., 2017. 10Be systematics in the Tsangpo-Brahmaputra catchment: the cosmogenic nuclide legacy of the eastern Himalayan syntaxis. *Earth Surf. Dyn.* 5, 429–449.

Malamud, B., Turcotte, D.L., Guzzetti, F., Reichenbach, P., 2004. Landslide inventories and their statistical properties. *Earth Surf. Process. Landf.* 29 (6), 687–711.

- Marc, O., Hovius, N., Meunier, P., Gorum, T., Uchida, T., 2016. A seismologically consistent expression for the total area and volume of earthquake-triggered landsliding. *J. Geophys. Res. Earth Surf.* 121, 640–663. <https://doi.org/10.1002/2015JF003732>.
- Marc, O., Meunier, P., Hovius, N., 2017. Prediction of the area affected by earthquake-induced landsliding based on seismological parameters. *Nat. Hazards Earth Syst. Sci.* 17, 1159–1175. <https://doi.org/10.5194/nhess-17-1159-2017>.
- Marc, O., Behling, C., Turowski, J.M., Illien, L., Roessner, S., Hovius, N., 2018a. Long-term erosion of the Nepal Himalayas by bedrock landslide erosion of the Nepal Himalayas by bedrock landsliding: the role of monsoons, earthquakes and giant landslides. *Earth Surf. Dyn. Discuss.* <https://doi.org/10.5194/esurf-2018-69.41pp>.
- Marc, O., Stumpf, A., Malet, J.-P., Gosset, M., Uchida, T., Chiang, S.-H., 2018b. Towards a global database of rainfall-induced inventories; first insights from past and new events. *Earth Surf. Dyn. Discuss.* <https://doi.org/10.5194/esurf-2018-20.28pp>.
- Mathur, L., 1953. Assam earthquake of 15th August 1950, a short note on factual observations. In: *A Compilation of Papers on the Assam Earthquake of August 15, 1950, Vol.1*. The Central Board of Geophysical Publisher, National Geophysical Research Institute, Hyderabad, India, pp. 56–60.
- Mishra, C., Datta, A., Madhusudan, M.D., 2004. The high altitude wildlife of Western Arunachal Pradesh: a survey report. In: *CERC Technical Report No. 8*. Nature Conservation Foundation, International Snow Leopard Trust, and Wildlife Conservation Society (India Program), Mysore, India.
- Mishra, R.L., Jayagondaperumal, R., Sahoo, H., 2016a. Active tectonics of Dikrong Valley, northeast Himalaya, India: Insight into the differential uplift and fold propagation from river profile analysis. *Himal. Geol.* 37 (2), 85–94.
- Mishra, R.L., Singh, I., Pandey, A., Rao, P.S., Sahoo, H.K., Jayagondaperumal, R., 2016b. Paleoseismic evidence of a giant medieval earthquake in the eastern Himalaya. *Geophys. Res. Lett.* 43 <https://doi.org/10.1002/2016GL068739>, 9pp.
- Misra, D.K., 2007. Geomorphic features along the active faults in the Lohit and Dibang valleys, Eastern Arunachal Pradesh, India. *Zeitschrift Geomorphol.* 51 (3), 327–336.
- Montgomery, D.R., Hallett, B., Yuping, L., Finnegan, N., Anders, A., Gillespie, A., Greenberg, H.M., 2004. Evidence for Holocene megafloods down the Tsangpo River gorge, southeastern Tibet. *Quat. Res.* 62, 201–207.
- Ouimet, W.B., Whipple, K.X., Royden, L.H., Sun, Z., Chen, Z., 2007. The influence of large landslides on river incision in a transient landscape: Eastern margin of the Tibetan Plateau (Sichuan, China). *GSA Bull.* 119 (1/12), 1462–1475.

Panda, R., Padhee, S.K., Dutta, S., 2014. GLOF study in Tawang River Basin, Arunachal Pradesh, India. In: The International Archives of the Photogrammetry, Remote Sensing and Spatial Information Sciences, Volume 15–8, ISPRS Technical

Commission 8th Symposium, 09–12 December 2014, Hyderabad, India, pp. 101–109.

Panda, S., Kumar, A., Das, S., Devrani, R., Rai, S., Prakash, K., Srivastava, P., 2020.

Chronology and sediment provenance of extreme floods of Siang River (Tsangpo-Brahmaputra River valley), northeast Himalaya. *Earth Surf. Process. Landf.* 45,

2495–2511.

Pandey, A., Dabral, P.P., Chowdary, V.M., Yadav, N.K., 2008. Landslide hazard zonation using remote sensing and GIS: a case study of Dikrong river basin, Arunachal Pradesh, India. *Environ. Geol.* 54, 1517–1529.

Pandey, A., Mathur, A., Mishra, S.K., Mal, B.C., 2009. Soil erosion modeling of a

Himalayan watershed using RS and GIS. *Environ. Earth Sci.* 59, 399–410. Pandit, M.K.,

Sodhi, N.S., Koh, L.P., Bhaskar, A., Brook, B.W., 2007. Unreported yet

massive deforestation driving loss of endemic biodiversity in Indian Himalaya. *Biodivers. Conserv.* 16, 153–163.

Portenga, E., Bierman, P., Duncan, C., Corbett, L.B., Kehrwald, N., Rood, D.H., 2015.

Erosion rates of the Bhutanese Himalaya determined by in-situ-produced <sup>10</sup>Be.

*Geomorphology* 233, 112–126.

Priyanka, R.S., Jayangondaperumul, R., Pandey, A., Mishra, R.L., Singh, I., Bhushan, R.,

Srivastava, P., Ramachandran, S., Shah, C., Kedia, S., Sharma, A.K., Bhat, G.R., 2017.

Primary surface rupture of the 1950 Tibet-Assam great earthquake along the eastern Himalayan front, India. *Sci. Rep.* 7, 5433. [https://doi.org/10.1038/s41598-017-](https://doi.org/10.1038/s41598-017-05644-y)

05644-y, 12pp.

Prokop, P., Poreba, G., 2012. Soil erosion associated with an upland farming system under population pressure in Northeast India. *Land Degrad. Dev.* 23, 310–321.

Ragendran, C.P., Rajendran, K., Duarah, B.P., Baruah, S., Earnest, A., 2004. Interpreting

the style of faulting and paleoseismicity associated with the 1897 Shillong, Northeast India, earthquake: Implications for regional tectonism. *Tectonics* 23, TC4009.

<https://doi.org/10.1029/2003TC001605>, 12pp.

Rawat, J.S., Joshi, R.C., 2012. Remote-sensing and GIS-based landslide-susceptibility zonation using the landslide index method in Igo River Basin, Eastern Himalaya, India. *Int. J. Remote Sens.* 33 (12), 3751–3767.

Rawat, J.S., Joshi, R.C., Mesia, M., 2013. Estimation of erosivity index and soil loss under different land uses in the tropical foothills of Eastern Himalaya (India). *Trop. Ecol.*

54 (1), 47–58.

Ray, K.B., 1956. Tista Flood Problem in West Bengal. *Econ. Polit. Wkly.* 19, 1956.  
Reddy, D.V., Nagabhushanam, P., Kumar, D., Sukhija, B.S., Thomas, P.J., Pandey, A.K.,

Sahoo, R.N., Prasad, G.V. Ravi, Datta, K., 2009. The great 1950 Assam earthquake revisited: field evidences of liquefaction and search for paleoseismic events. *Tectonophysics* 474, 463–472.

Reid, L.M., Dunne, T., 2016. Sediment budgets as an organizing framework in fluvial geomorphology. In: Kondolf, M., Piégay, H. (Eds.), *Tools in Fluvial Geomorphology*, Second edition. John Wiley and Sons, pp. 357–379. Chapter 16.

Riba, J., Joshi, R.C., 2014. The Eastern Himalaya. Soil loss estimation of Kale River basin, Arunachal Pradesh. In: Sharma, S., Phartiyal, P., Pant, P.D. (Eds.), *Himalayan Vulnerability*. Uttarakhand 2013. Central Himalayan Environment Association, Nainital, India, pp. 73–81.

Ring, U., Brandon, M.T., Willett, S.D., Lister, G.S., 1999. Exhumation processes. In: Ring, U., Brandon, M.T., Lister, G.S., Willett, S.D. (Eds.), *Exhumation Processes: Normal Faulting, Ductile Flow and Erosion*, vol. 154. Geological Society, London, Special Publications, pp. 1–27.

Rosenkranz, R., Schildgen, T., Wittmann, H., Spiegel, C., 2018. Coupling erosion and topographic development in the rainiest place on Earth: Reconstructing the Shillong Plateau uplift history with in-situ cosmogenic <sup>10</sup>Be. *Earth Planet. Sci. Lett.* 483, 39–51.

Salvi, D., Mathew, G., Kohn, B., 2017. Rapid exhumation of the upper Siang Valley, Arunachal Himalaya since the Pliocene. *Geomorphology* 284, 238–249.

Sarkar, M.H., Thorne, C.R., 2006. Morphological response of the Brahmaputra-Padma-Lower Meghna river system to the Assam earthquake of 1950. In: Smith, G.H.S., Best, J.L., Bristow, C.S., Petts, G.E. (Eds.), *Braided Rivers. Process, Deposits, Ecology and Management*, Special Publication of the International Association of Sedimentologists, No. 36. Blackwell, Oxford, pp. 289–310.

Sarma, J.N., 2005. Fluvial processes and morphology of the Brahmaputra River in Assam, India. *Geomorphology* 70, 226–256.

Sarma, J.N., Acharjee, S., 2018. A study on variation in channel width and braiding intensity of the Brahmaputra River in Assam, India. *Geosciences* 8, 343. <https://doi.org/10.3390/geosciences8090343>, 19pp.

Shang, Y., Yang, Z., Li, L., Liu, D., Liao, Q., Wang, Y., 2003. A super-large landslide in Tibet in 2000: background, occurrence, disaster and origin. *Geomorphology* 54, 225–243.

Shi, X., Zhang, F., Lu, X.X., Wang, Z., Gong, T., Wang, G., Zhang, H., 2017.

Spatiotemporal Variations of Suspended Sediment Transport in the Upstream and Midstream of the YarlungTsangpo River (the Upper Brahmaputra). *Earth Surface Processes and Landforms, China*. <https://doi.org/10.1002/esp.4258>.

Shrestha, A.B., Agrawal, N.K., Alftnhan, B., Bajracharya, S.R., Mar´echal, J., van Oort, B. (Eds.), 2015. *The Himalayan Climate and Water Atlas: Impacts of Climate Change on Water Resources in Five of Asia’s Major River Basins*. ICIMOD, GRID-Arendal and CICERO.

Singh, S.K., 2006. Spatial variability in erosion in the Brahmaputra basin: causes and impacts. *Curr. Sci.* 90 (9), 1272–1276.

Singh, A.K., France-Lanord, C., 2002. Tracing the distribution of erosion in the Brahmaputra watershed from isotopic compositions of stream sediments. *Earth Planet. Sci. Lett.* 202, 645–662.

Srivastava, P., Mishra, D.K., 2008. Morpho-sedimentary records of active tectonics at the Kameng river exit, NE Himalaya. *Geomorphology* 96, 187–198.

Srivastava, S., Singh, T.P., Singh, H., Kushwaha, S.P.S., Roy, P.S., 2002. Assessment of large-scale deforestation in Sonitpur district of Assam. *Curr. Sci.* 82 (12), 1479–1484.

Srivastava, P., Bhakuni, S.S., LuireI, K., Misra, D.K., 2008. Morpho-sedimentary records at the Brahmaputra River exit, NE Himalaya: climate-tectonic interplay during the late Pleistocene-Holocene. *J. Quat. Sci.* 24 (2), 175–188.

Srivastava, P., Kumar, A., Chaudhary, S., Meena, N., Sundriyal, Y.P., Rawat, S., Rana, N., Perumal, R.J., Bisht, P., Sharma, R., Bagri, D.S., Juyal, N., Wasson, R.J., Ziegler, A. D., 2017. Paleofloods records in Himalaya. *Geomorphology* 284, 17–30.

Starkel, L., Basu, S., 2000. *Rains, Landslides and Floods in the Darjeeling Himalaya*. Indian National Science Academy, 168pp.

Stewart, R.J., Hallet, B., Zeitler, P.K., Malloy, M.A., Allen, C.M., Trippett, D., 2008. Brahmaputra sediment flux dominated by highly localized rapid erosion from the easternmost Himalaya. *Geology* 36 (9), 711–714.

Tanyas, H., Kirschbaum, D., Go`rüm, T., Westen, C.J., Tang, C., Lombardo, L., 2021. A closer look at factors governing landslide recovery time in post-seismic periods. *Geomorphology*. <https://doi.org/10.1016/j.geomorph.2021.107912>.

Tewari, P., 2004. A study on Soil Erosion in Pasighat Town (Arunachal Pradesh) India. *Nat. Hazards* 32, 257–275.

Turzewski, M.D., Huntington, K.W., Le Veque, R.J., Feathers, J.K., Larsen, I.J., Montgomery, D.R., 2014. Megaflood erosion of the Tsangpo Gorge constrained by

hydraulic modeling, geochronology, and geochemical fingerprinting. In: American Geophysical Union, Fall Meeting 2014 abstract #EP13A-3506.

Wang, P., Scherler, D., Liu-Zeng, J., Mey, J., Avouac, J.-P., Zhang, Y., Shi, D., 2014. Tectonic control of YarlungTsangpo Gorge revealed by a buried canyon in Southern Tibet. *Science* 346, 978–981.

Wasson, R.J., 2008. In: Sanchez, I.B., Alonso, C.L. (Eds.), *Upland Deforestation, Erosion, and Downstream Impacts. Deforestation Research Progress*. Nova Science Publications, pp. 51–65. Chapter 4.

Wasson, R.J., Juyal, N., Jaiswal, M., McCulloch, M., Sarin, M.M., Jain, V., Srivastava, P., Singhvi, A.K., 2008. The mountain-lowland debate: deforestation and sediment transport in the upper Ganga catchment. *J. Environ. Manag.* 88, 53–61.

Wasson, R.J., Saikia, A., Bansal, P., Chuah, C.J., 2020. Flood Mitigation, climate change adaptation, and technological lock-in in Assam. *Ecol. Econ. Soc. INSEE J.* 3 (2), 83–104.

Whipple, K.X., 2014. Can erosion drive tectonics? *Science* 364, 918–919.

Yang, W., Fang, J., Liu-Zhang, J., 2021. Landslide-lake outburst floods accelerate downstream slope slippage. *Earth Surf. Dyn.* <https://doi.org/10.5194/esurf-2021-14>.

Yhoshu, K., Krishnaiah, Y.V., 2017. Evaluation of landslide hazard of Kohima, India.

Coordinates. November 2017. <https://mycoordinates.org/evaluation-of-landslide-hazard-of-kohima-india/>.

Zhang, J.Y., Yin, A., Liu, W.C., Wu, F.Y., Lin, D., Grove, M., 2012. Coupled U-Pb dating and Hf isotopic analysis of detrital zircon of modern river sand from the Yalu River (YarlungTsangpo) drainage system in southern Tibet: Constraints on the transport processes and evolution of Himalayan rivers. *Geol. Soc. Am. Bull.* 124 (9/10), 1449–1473.

Zhang, X.-L., Cui, L.-F., Xu, S., Liu, C.-Q., Zhao, Z.-Q., Zhang, M.-L., Liu-Zeng, J., 2021.

Assessing non-steady-state erosion processes using paired  $^{10}\text{Be}$  –  $^{26}\text{Al}$  in South- Eastern Tibet. *Earth Surf. Process. Landf.* 46, 1363–1374.



## Tables

Table 1

Summary of the estimates of percentages of the Brahmaputra River sediment flux near to its passage into Bangladesh that comes from the Gorge.

| Method  | Tibet | Siang River@ | Mishmi Hills | Himalaya (also known to as north bank tributaries) | Shillong Plateau | Indo-Burman Ranges | Sources                                      |
|---|-------|--------------|--------------|--|------------------|--------------------|--|
| Bulk sand petrography and geochemistry        |       | 41           | 24           | 23   | 11               | 1                  | Garzanti et al. (2004)                       |
| Geochemistry, suspended load and some bedload | 5     | 45           | 10           | 40   |                  |                    | Singh and France-Lanord (2002); Singh (2006) |
| <sup>10</sup> Be                              | 12    | 30           | 22           | 36   |                  | <1                 | Lupker et al. (2017)                         |
| Detrital zircons thermochronology             |       | 50#          |              |  |                  |                    | Stewart et al. (2008)                        |
| Sand petrography                              |       | 35-51        |              |  |                  |                    | Gerignani et al. (2018)                      |
| Gauging                                       | 5     | 32           |              |  |                  |                    | Goswami (1985)                               |

# Probably too high as it takes no account of dilution by downstream tributaries.

@ This includes both the NB-GP massif, the Gorge and the valley of the Siang River downstream.

Table 2

Best estimates of proportionate contributions to the main river from the various source regions. Note that the proportions do not add to 100% because of uncertainties, Also the relative quantities from the various processes are not known but landslides are likely to be the largest contributor.

| Source region      | Sediment contribution (%) <sup>1</sup> | Major processes <sup>2</sup> |
|--------------------|--|------------------------------|
| Tibetan Plateau    | <1                                     | S,R,L,W                      |
| Syntaxis           | 45                                     | L,I,G,Lo                     |
| Mishmi Hills       | 10                                     | L, Lo, G, S,R, Ro, I, W, C   |
| Himalaya           | 40                                     | L, Lo, G, S, R, Ro, W, C, I  |
| Indo-Burman Ranges | 1                                      | L, Lo, S, R, Ro, I           |
| Shillong Plateau   | 11                                     | I, L, S                      |

<sup>1</sup> To the river as it enters Bangladesh.

<sup>2</sup> S-sheet and rill erosion; R-Riverbank Erosion, not necessarily with river widening; L-Landslides; G-GLOFs- Lo-LLOFs; Ro-roads; I-river incision. W-river widening. C- channel relocation.

Figures

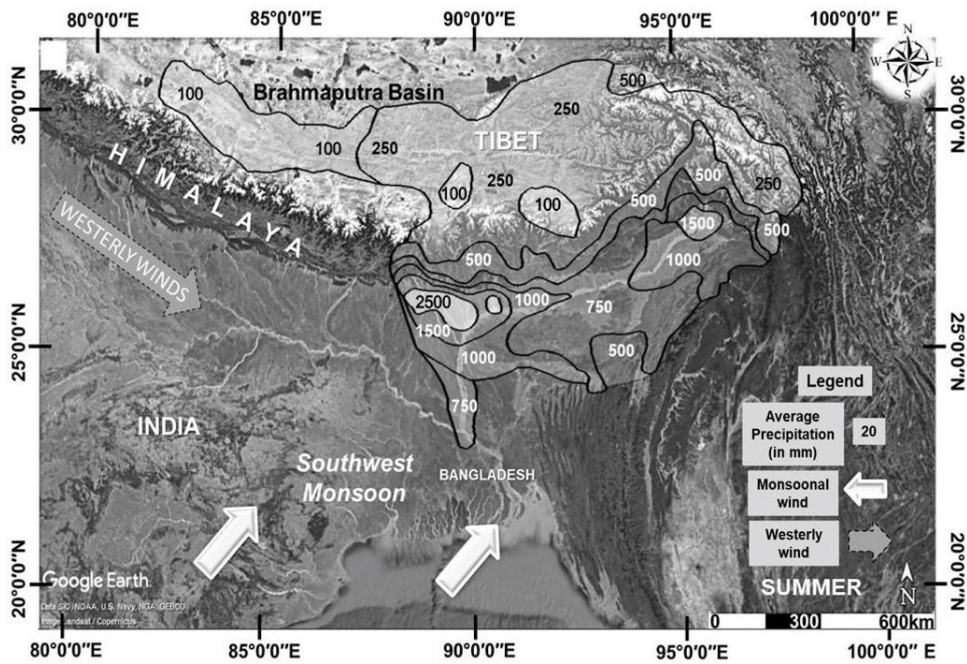


Fig. 1. Average total precipitation from the Southwest Monsoon 1981–2007 (after Shrestha et al., 2015) overlain on a Google Earth™ image.

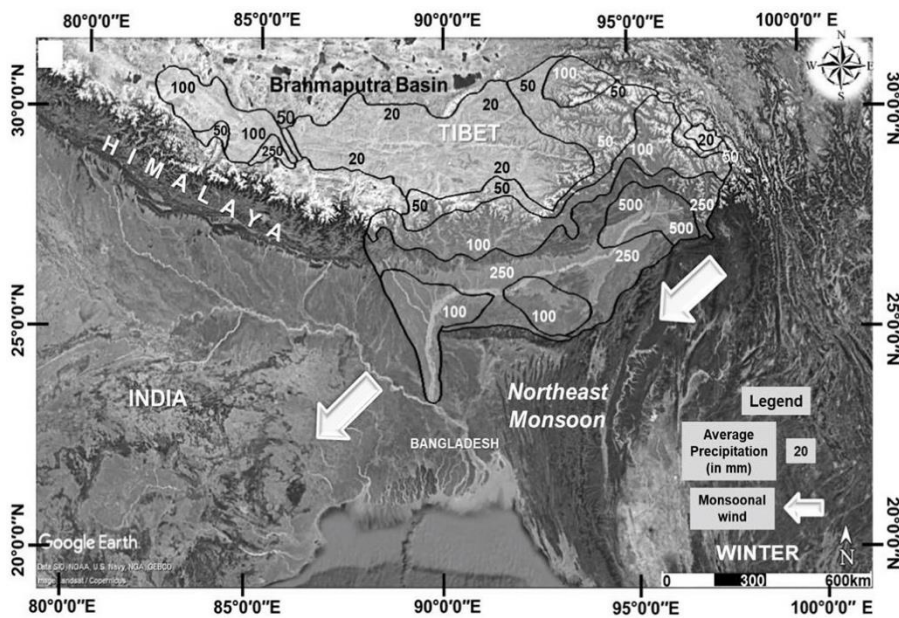
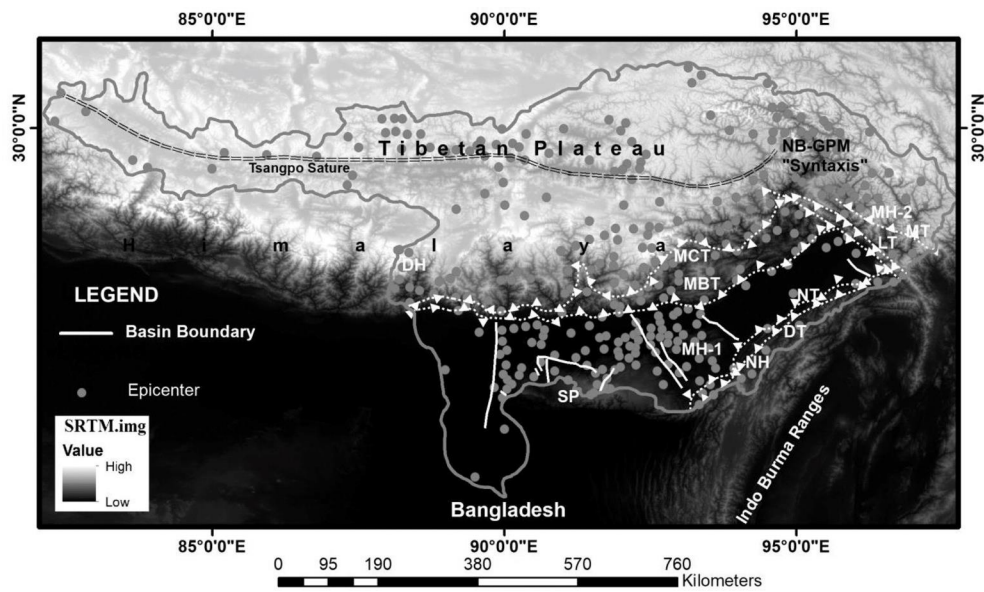


Fig. 2. Average total precipitation from the Northeast Monsoon 1981–2007 (after Shrestha et al., 2015) overlain on a Google Earth™ image



- |   |                                   |
|---|-----------------------------------|
| <b>MH-1= Mikir Hills</b>                                  | <b>MCT = Main Central Thrust</b>  |
| <b>MH-2= Mishmi Hills</b>                                 | <b>MBT = Main Boundary Thrust</b> |
| <b>NH = Naga Hills</b>                                    | <b>NT = Naga Thrust</b>           |
| <b>SP = Shillong Plateau</b>                              | <b>DT = Disang Thrust</b>         |
| <b>DH = Darjeeling Himalaya</b>                           | <b>MT = Mishimi Thrust</b>        |
| <b>NB-GPM "Syntaxis" = Namcha Barwa-Gyala Peri Massif</b> | <b>LT = Lohit Thrust</b>          |

Fig. 3. Location map showing the major sediment source regions, main faults, and litho-tectonic terrains.

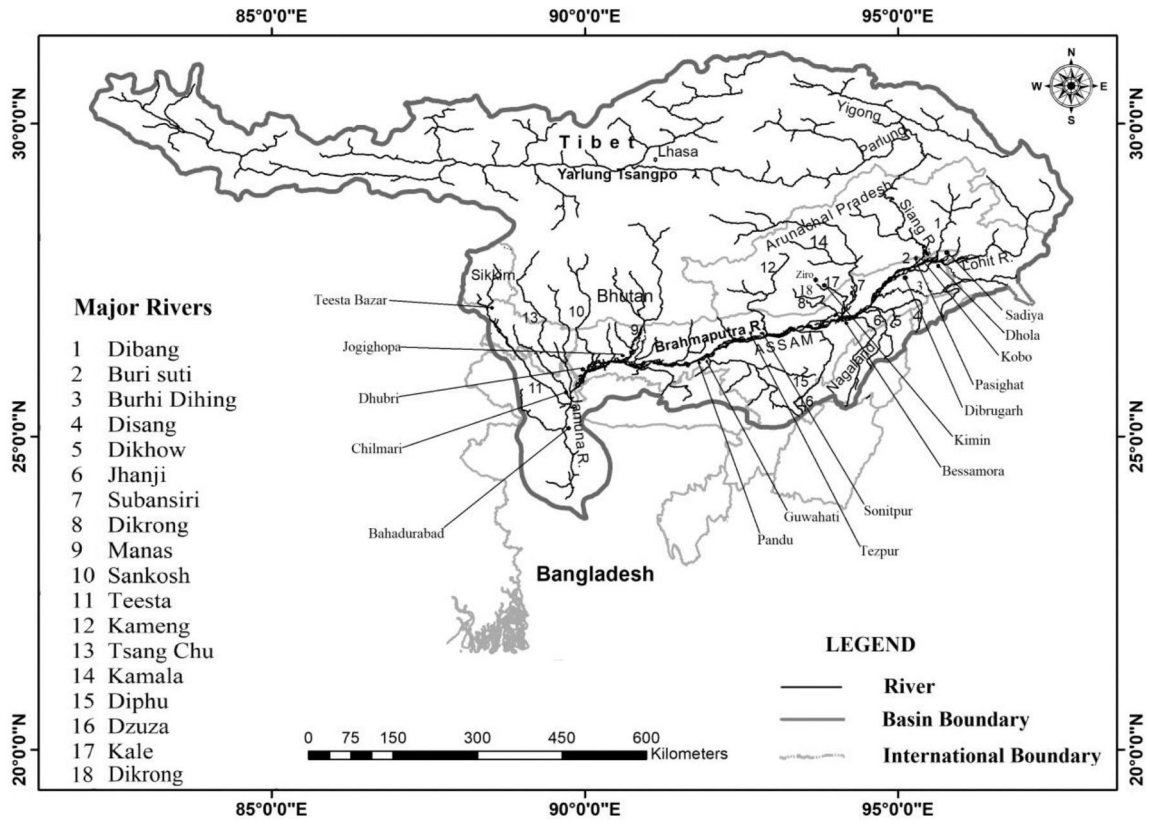


Fig. 4. Locations of the major rivers and towns mentioned in the text.

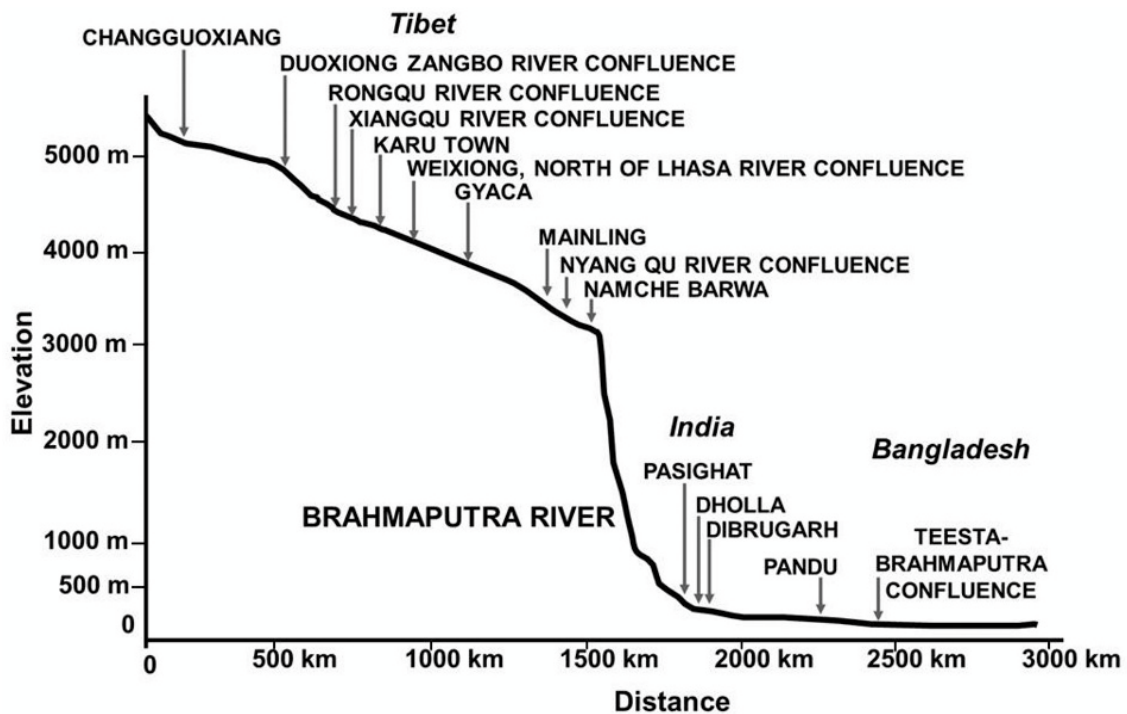


Fig. 5. Long-profile of the Brahmaputra River with key locations. Source: data from Sarma (2005) using ASTER GDEM (30 m resolution) to rectify locations.

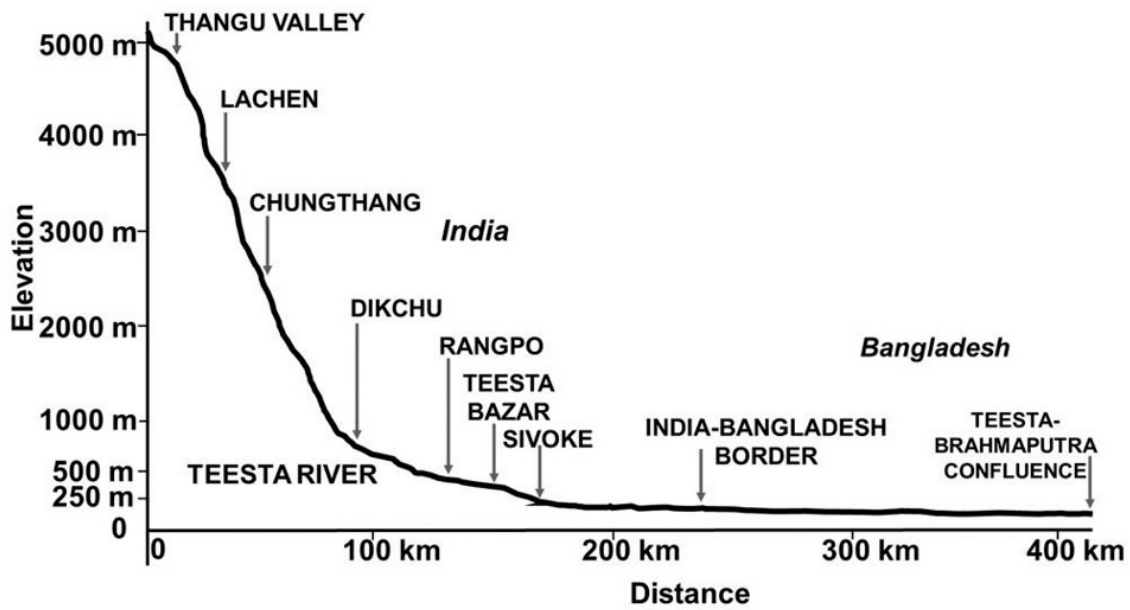


Fig. 6. Long-profile of the Teesta River with key locations. Source: ASTER GDEM (30 m resolution).

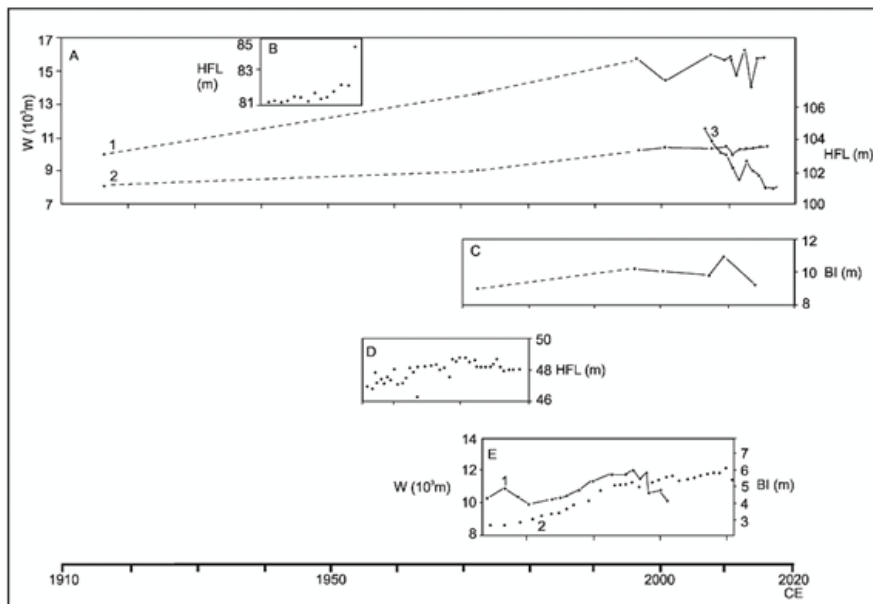


Fig. 7. Time series of key Brahmaputra channel variables. A1-mean channel width at Dibrugarh (from Sarma and Acharjee, 2018). A2 is High Flood Level (HFL) at Dibrugarh (from Sarma and Acharjee, 2018). A3 is HFL at Dholla (data from Assam Department of Water Resources). B-HFL on the Teesta (from Ray, 1956). C-Braid Index at Dibrugarh (from Sarma and Acharjee, 2018). D-HFL at Pandu (from Goswami, 1985, and Sarkar and Thorne, 2006) E1-BI Jamuna (from Sarker and Thorne, 2006, as the average of the Upper and Lower reaches. E2-mean width of the Jamuna River in Bangladesh (from Sarkar and Thorne, 2006).

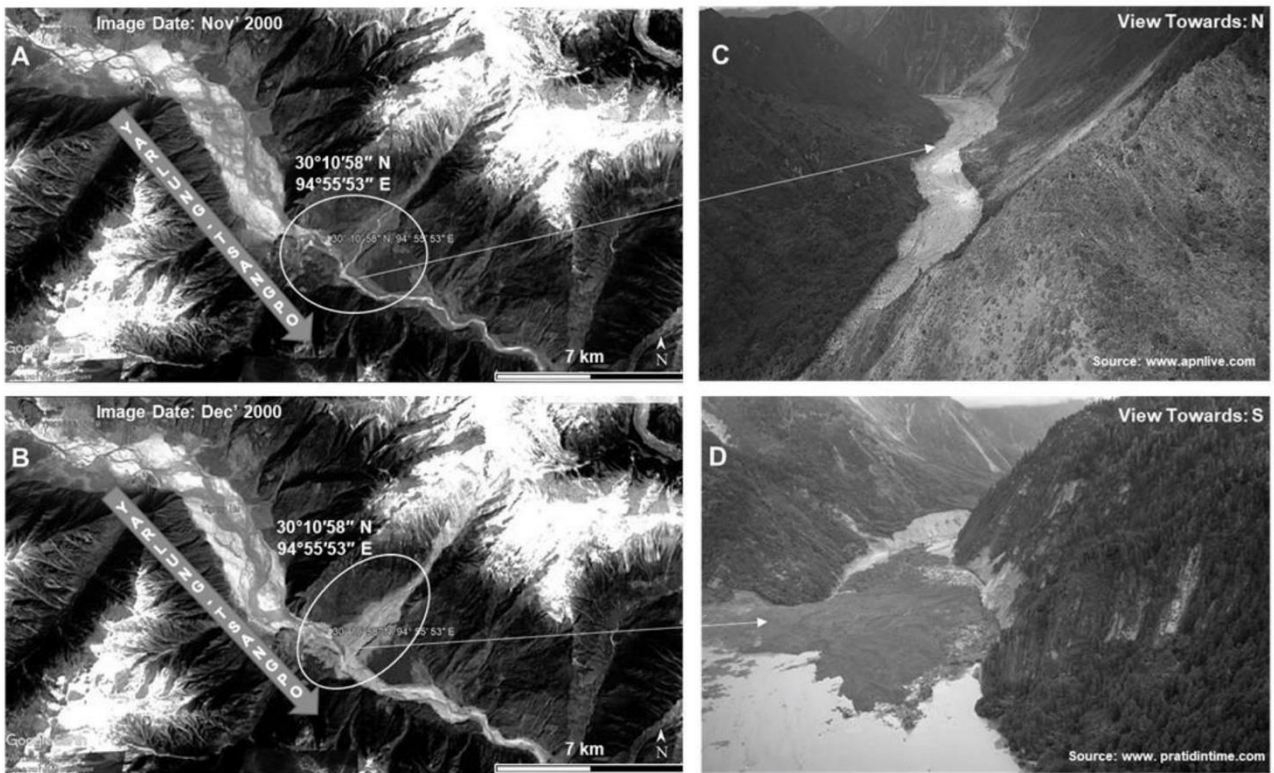


Fig. 8. Example of a large LLOF causing event at Zhamu Creek near the confluence with the Yarlung-Tsangpo in the eastern TP in May 2000. Google Earth™ images (A and B) show the location and low altitude oblique views, from [www.apnlive.com](http://www.apnlive.com) and [www.pratidintime.com](http://www.pratidintime.com) for C and D respectively, show details of the dam.

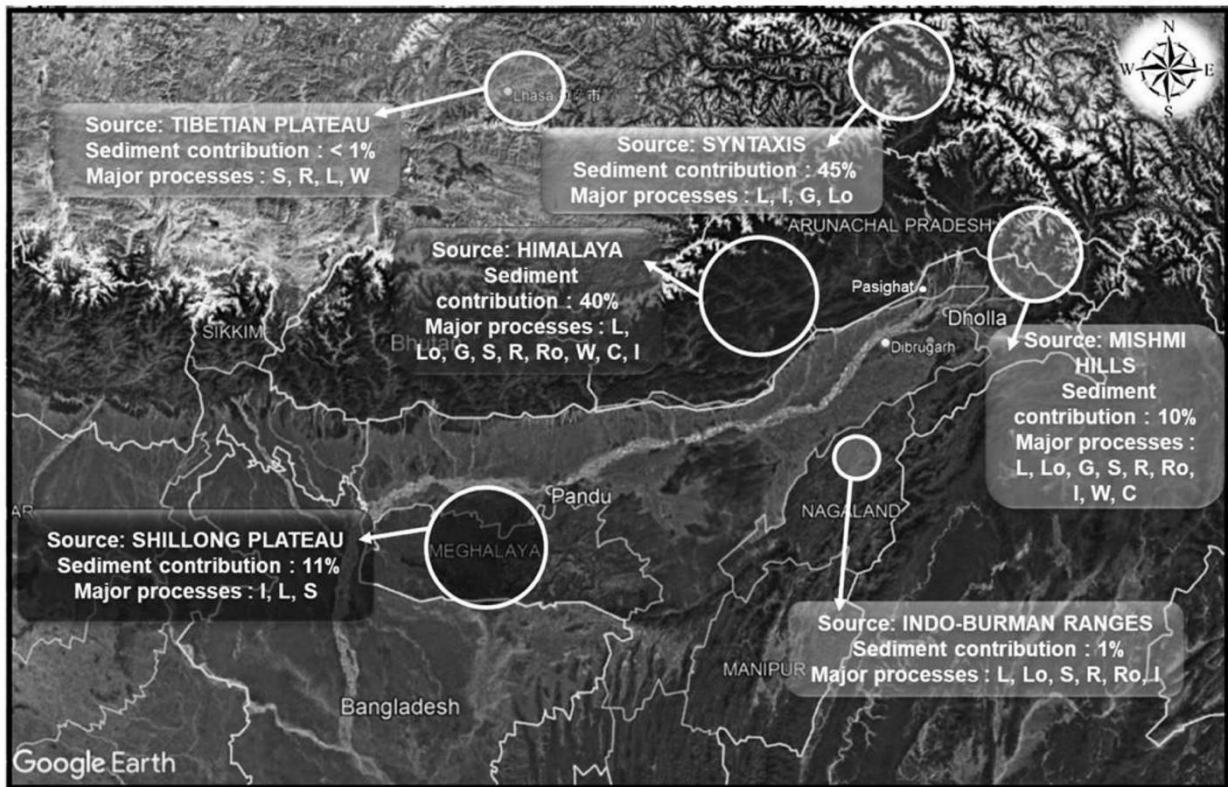


Fig. 9. The information in Table 2 shown spatially on a Google Earth™ image.